NACA

RESEARCH MEMORANDUM

TWO-DIMENSIONAL CHORDWISE LOAD DISTRIBUTIONS

AT TRANSONIC SPEEDS

By Walter F. Lindsey and Richard S. Dick

Langley Aeronautical Laboratory
Langley Field, Va.

NATIONAL ADVISORY COMMITTEE
FOR AERONAUTICS
WASHINGTON

February 18, 1952
Declassified September 13, 1957
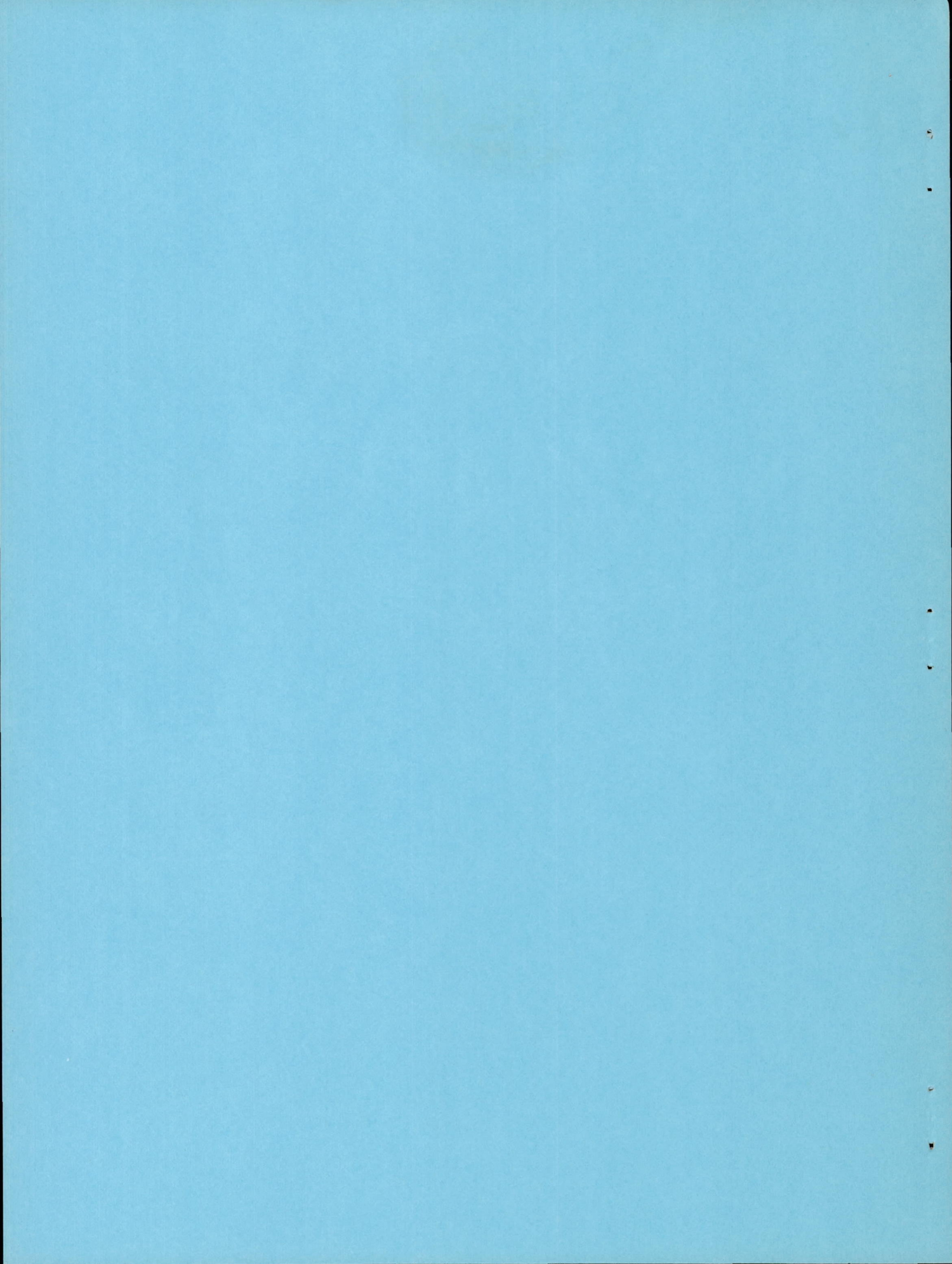
NATIONAL ADVISORY COMMITTEE FOR AERONAUTICS

RESEARCH MEMORANDUM

TWO-DIMENSIONAL CHORDWISE LOAD DISTRIBUTIONS

AT TRANSONIC SPEEDS

By Walter F. Lindsey and Richard S. Dick

SUMMARY

From tests on the NACA 16-009 airfoil and on eight airfoils of the
NACA 6A series, results are presented to show that the chordwise loading
due to lift at a Mach number of 1.0 is insignificantly affected by thick-
ness distribution within the range of airfoil shapes presented and only
slightly affected by thickness. In addition, a method of estimating the
pressure distributions for lifting symmetrical airfoils at a Mach number
of 1.0 which seems applicable to profiles of the type considered herein
is presented. The possibility is indicated that the effects of camber,
thickness, and angle of attack may be treated separately at a Mach number
of 1.0 as they are at low subsonic Mach numbers and at supersonic Mach
numbers.

INTRODUCTION

The chordwise loadings on airfoils in incompressible two-dimensional
flow can be predicted by available theoretical means to a high degree of
accuracy at moderate angles of attack and lift coefficients where the
effects of viscosity are small (references 1 and 2). The changes in
loading due to the effects of compressibility can be estimated by simple
velocity-correction formulas such as those derived in papers by Prandtl
and Glauert, Kármán and Tsien, Kaplan and Garrick, and others. Generally,
as a result of assumptions used in the derivations, the velocity-correction
formulas are limited in application to purely subsonic or subcritical
flow. Comparisons at subcritical Mach numbers between experimentally
determined loadings and the loadings derived theoretically, with the
effect of compressibility estimated by velocity-correction formulas, show
agreement within sufficient accuracy for usual engineering purposes.

At supercritical or low transonic Mach numbers, the occurrence of
both subsonic and supersonic regions of flow, together with shocks and

flow separation, has seriously handicapped theoretical treatment of the problem; as a consequence, experimental investigations have been relied upon as the main source of information. These investigations, in general, have been limited to Mach numbers of less than 0.9 because of usual wind-tunnel limitations. The recent use of revised equipment and test techniques, such as the annular transonic tunnel (reference 3) and the adoption of the open-throat testing technique (reference 4), have permitted data to be obtained at Mach numbers approaching 1.0.

The purpose of the present paper is to discuss two-dimensional loadings at Mach numbers between 0.8 and 1.0 obtained from pressure-distribution measurements in the Langley 4- by 19-inch semiopen tunnel. The basic-airfoil-profile variables that are considered in the discussion are thickness, thickness distribution, and camber.

SYMBOLS

c	airfoil chord
c_l	section lift coefficient
$c_{m_{c/4}}$	section pitching-moment coefficient about quarter-chord axis
k	a profile shape factor
M	Mach number
n	an exponent
p	static pressure
P	pressure coefficient $\left(\dfrac{p_{local} - p_{stream}}{q} \right)$
ΔP	P for lower surface minus P for upper surface at a given chordwise station
q	free-stream dynamic pressure
t	airfoil maximum thickness
Δ	incremental value
ν	angle of supersonic flow expansion

Subscripts:

t   thickness at any chordwise station

max   maximum value

APPARATUS AND TESTS

The tests were conducted in the Langley 4- by 19-inch semiopen
tunnel (fig. 1), which is an induction tunnel housed within an enclosure
to minimize condensation problems. (Enclosure discussed in reference 5.)
The 4-inch dimension of the tunnel is formed by two parallel steel plates,
whereas the 19-inch dimension is the dimension of the open jet, the top
and bottom chambers of which are connected by a duct. Velocity distri-
butions in the test region obtained from static-pressure measurements
at the tunnel walls are shown in figure 2. Figure 2(a) shows that the
velocities along the longitudinal axis at the model location are within
±1 percent for stream Mach numbers around 0.8. For stream Mach numbers
near 1.0, the velocities are within ±2 percent. The velocity gradients
along the normal-to-chord axis (fig. 2(b)) are smaller.

Each airfoil completely spanned the test section along the 4-inch
dimension of the tunnel and was supported by large circular end plates
which fitted into the tunnel walls and rotated with the model to retain
continuity of the surfaces of the tunnel walls. The juncture between
airfoil and tunnel wall was sealed.

The investigation included schlieren photographs of the flow and
static-pressure-distribution measurements on the airfoils. Approximately
40 static-pressure orifices were installed in two rows 0.25 inch on
either side of the center line of the models. Test runs were made at
constant angles of attack through a Mach number range. The stream Mach
number was controlled by regulating the mass flow through the tunnel
by using a sonic-throat device, designated "choker" in figure 1, located
downstream of the test section.

Variations in airfoil thickness were investigated by using the
NACA 64A-series profile, varying in thickness from 4 to 12 percent of
chord (fig. 3(a)). Effects of thickness distribution were investigated
by tests on the NACA 6A- and 16-series profiles having a constant thick-
ness of 9 percent (fig. 3(b)). The extent of the investigation on camber
was limited to tests on 6-percent-thick airfoils of the NACA 64A series
varying in camber from zero to a design lift coefficient of 0.5
(fig. 3(c)). The test Reynolds number of these 4-inch-chord airfoils
at a Mach number of 1.0 was 1.6×10^6.

PRECISION OF DATA

The test data indicated by the scatter of test points that the error in lift coefficient was within ±0.007. In a similar comparison, the maximum error in pressure coefficient was approximately ±0.005.

Data obtained in the semiopen test section are subject to jet-boundary corrections (reference 6). The theoretical corrections (reference 6) for the data c_l, P, and M presented herein are negligible at Mach numbers around 0.8. At Mach numbers near 1.0 the corrections are indeterminate, since they include $1 - M^2$ terms. The only available means of determining the validity of the data at sonic velocities is by direct comparisons of these data with data obtained from other facilities, or by different techniques.

Pressure-distribution measurements on two models tested in the annular transonic tunnel (reference 3) and in the 4- by 19-inch tunnel are compared in figure 4. Data for the NACA 65-110 airfoil from unpublished flight tests of the X-1 airplane, in which measurements of the pressure distribution along the midsemispan of the wing were made, are presented in figure 4(a). The comparison of the data in figure 4(a) shows very good correlation between the 4- by 19-inch tunnel data and flight results. In a comparison of data obtained from the annular transonic and 4- by 19-inch tunnels on a symmetrical-wedge airfoil at a Mach number of 1.0 at zero lift coefficient (fig. 4(b)), good agreement was obtained not only between the two facilities, but also between the two sets of experimental results and the theoretical results of reference 7. The good correlation of these pressure distributions in figures 4(a) and 4(b) indicates that the data obtained from the 4- by 19-inch semiopen tunnel at a Mach number of 1.0 are representative of the flows obtained in free air.

RESULTS AND DISCUSSION

Experimental Loading on Symmetrical Airfoils

Effect of thickness.- The effect of thickness on the flow past airfoils at a lift coefficient of 0.2 and at Mach numbers between 0.8 and 1.0 is shown by the schlieren photographs in figure 5. At a Mach number of 0.82, figure 5(a) shows that the shock is more rearwardly located on the upper surface of the thicker profile than on the thinner profile. The rearward location of the shock and the large curvature of the airfoil produce higher local Mach numbers in front of the shock and, consequently, a stronger shock as is evidenced by the appearance of the

shock and the flow separation that occurs near the foot of the shock on
the thick profile. Increasing the Mach number to 0.91 (fig. 5(b)) causes
the shocks to move to approximately the same chordwise location on the
upper surfaces of the two profiles. On the thin body there is a small
amount of separation, whereas on the thick body the vertical extent of
separation is quite large. The lower-surface shock on the 12-percent-
thick body is located more rearwardly than is the upper-surface shock.
These shock locations on the 12-percent-thick profile are expected to
produce downloads on the airfoil in the vicinity of the trailing edge.
Further increase in Mach number to 1.0 (fig. 5(c)) causes the shocks to
move to the trailing edge and eliminates shock-induced separation. Fig-
ure 5 has, in general, shown that pressure discontinuities resulting from
shocks on the airfoils are eliminated around a Mach number of 1.0 because
the shocks have moved back to or past the trailing edge.

The measured chordwise loadings on symmetrical airfoils are pre-
sented as the difference in pressure coefficients between the lower and
upper surfaces at given chordwise stations divided by the section lift
coefficient $\Delta P/c_l$. This form of loading factor minimizes the effects
of changes in lift coefficient and permits comparisons to be made of
loadings at different lift coefficients. The effects of thickness on
the measured chordwise loadings are shown in figure 6 for NACA 64A-series
airfoils having thicknesses of 4-, 6-, 9-, and 12-percent chord at various
Mach numbers. At a Mach number of 0.81, the 9- and 12-percent-thick
profiles show some evidence of shock on the loading around the 60-percent-
chord station. When the Mach number is increased to 0.91, a large reverse
loading occurs on the 12-percent-thick airfoil between the 50- and
80-percent-chord stations; this loading is attributable to flow separation
and a more rearward location of the lower-surface shock, as was seen in
the flow photograph (fig. 5(b)). At this Mach number the thinner pro-
files of 4 and 6 percent thickness also show shock effects on the loading.
As the Mach number is increased to 0.97, the shocks move toward the
trailing edge and the accompanying separation observed in flow studies
produced reversals of loading for the 9- and 12-percent-thick profiles.
At a Mach number of 1.0, no pronounced shock effects on the loadings are
present and the results indicate that thickness has only a small effect
on loading. A careful examination indicates that the loading becomes
somewhat larger at the leading edge and smaller at the trailing edge with
increase in thickness. These changes with thickness, however, are small.

Effect of thickness distribution.- Variations in thickness distri-
butions are represented by 9-percent-thick airfoils of the NACA 63A,
64A, 65A, and 16 series. These airfoils have their maximum thicknesses
located at the 36-, 39-, 42-, and 50-percent-chord stations, respectively.
The effects of thickness distribution on the flow past airfoils at Mach
numbers between 0.8 and 1.0 and lift coefficients around 0.17 are shown
by the schlieren photographs in figure 7. At a Mach number of 0.82,

figure 7(a) shows that moderately strong shocks are occurring around the 60-percent-chord station on the NACA 6A-series airfoils. The shock is located slightly more rearward on the 65A-series airfoil than on the 63A-series airfoil. On the NACA 16-series airfoil, near the 40-percent-chord station, a weak shock occurs which does not contribute to flow separation.

At a Mach number of 0.92, shown in figure 7(b), the upper-surface shocks on all the airfoils are accompanied by flow separation and the lower-surface shocks are generally rearward of the upper-surface shocks. The rearward displacement of the lower-surface shocks for these airfoils in combination with the flow separation on the upper surface contributes to negative loadings near the trailing edge, as was observed for the 12-percent-thick airfoils (figs. 5(b) and 6). Further examination of figure 7(b) shows that the chordwise extent of the reversals may be expected (at M = 0.92) to be somewhat larger on the 6A-series airfoils than on the 16 series, since the shocks on upper and lower surfaces of the 16-series airfoil are located much more closely to the trailing edge. At a Mach number of 1.0, figure 7(c) shows that the shocks have moved back to or off the trailing edges of the airfoils, as was observed for the airfoils of various thicknesses (fig. 5).

The chordwise loadings for these profiles at the various Mach numbers are shown in figure 8. At a Mach number of 0.82, lift coefficient approximately 0.23, the load distributions along the chord of the NACA 6A-series airfoils are quite similar. The three airfoils exhibit a rapid decrease in load between the 50- and 60-percent-chord stations corresponding to the location of the moderately strong shocks shown in figure 7(a). On the 16-series airfoil, no effects of the weak shock (shown in fig. 7(a)) are indicated in the load distribution. The reverse loading observed near the trailing edge on the 16-series profile at Mach number of 0.82 is a result of a forward location of the maximum velocity on the upper surface and a rearward location of maximum velocity on the lower surface. (These are comparable with upper-surface-shock and lower-surface-disturbance positions in fig. 7(a).)

When the Mach number is increased to 0.92 (fig. 8), the load distributions for the NACA 6A-series airfoils are still similar and exhibit a rapid decrease in load near the 50-percent-chord station, followed by a second rapid decrease around the 70-percent-chord station. The first decrease in load is attributed to effects of flow separation on the upper surface, whereas the second rapid decrease which produces a large negative load near the trailing edge is a result of the rearward location of the lower-surface shock. Similar effects are noted in the loading for the 16-series airfoil; however, the magnitude of the changes is smaller, primarily as a result of the decreased chordwise extent of influence of these effects as was anticipated from examination of the flow photographs in figure 7(b).

At a Mach number of 0.97 (fig. 8), the loadings for the various air-
foils are approximately the same except behind the 90-percent-chord
station. At a Mach number of 1.0, there are no systematic variations
in loading with thickness distribution and the differences between the
loadings are small. It appears, therefore, that a general loading curve
for Mach number 1.0 could be derived from the loadings presented and
that loading would, to a first approximation, be independent of thick-
ness and less dependent on thickness distribution within the range of
variables and conditions presented.

A general loading at a Mach number of 1.0, derived from an average
of the symmetrical-airfoil loadings of figures 6 and 8, is shown in
figure 9. In addition to the average loading obtained at lift coef-
ficients around 0.2, data on various profiles are included in figure 9
for lift coefficients between 0.52 and 0.68. Within the general spread
of the test data, the average loading curve appears to be applicable for
these higher lift coefficients.

Method of Estimating Pressure Distribution

The generality of the result obtained for angle-of-attack loading
suggests the possibility of a semiempirical method for predicting
symmetrical-airfoil pressure distributions at sonic speed. In such a
method the lifting pressures, which are considered independent of pro-
file shape, would be divided evenly between upper and lower surfaces
and added to the zero-lift pressure distribution in a manner analogous
to the incompressible case. The first step in such a procedure, however,
requires a knowledge of the distribution of pressures along the chord
for the no-lift or zero-angle-of-attack case. Methods of approach for
the zero-angle-of-attack determination of the pressure distributions
are: the continuation of the low-speed extrapolation methods to a Mach
number of 1.0, a special determination of the flow conditions at Mach
number 1.0, and a downward extrapolation with Mach number of the distri-
butions that would be expected at a supersonic speed.

Low-speed methods.- Various methods have been proposed whereby
pressure distributions at Mach numbers somewhat in excess of the critical
Mach number might be predicted (references 8, 9, and 10). At a Mach
number of 0.8 (0.2 above critical) the pressure distributions predicted
by these methods diverge widely from experiment, as illustrated by fig-
ure 10, for an airfoil similar to those tested in the present investi-
gation. These methods can be considered as an application of velocity-
correction formulas involving $1 - M^2$ terms. As a consequence, they
become indeterminate as the Mach number approaches 1.0 and, therefore,
none of these methods are applicable to the problem of determining the
flow at sonic stream velocity.

Sonic-speed methods.- The theoretical determination of the pressure
distribution on nonlifting symmetrical profiles at sonic speed is an
involved mathematical problem. Solutions have been given by Guderley
and Yoshihara (references 7 and 11) for two special profiles, a wedge
and a cusp-shaped profile. The theoretical solution for the wedge pro-
file at zero lift is in excellent agreement with experimental data (fig-
ure 4(b)). The method in its present form, however, is quite complicated
and further development of the theory is required before it can be
applied to round-edge profiles. For engineering purposes a simplified
method is needed.

The transonic similarity laws have been presented by von Kármán
for use in extrapolating force and pressure data with Mach number and
with thickness in the sonic speed range (reference 12; also, see refer-
ence 13). At a given Mach number, for example, the pressure coefficient
is proportional to thickness-chord ratio to the 2/3 power. The effect
of thickness on experimental pressure coefficients at the maximum-
thickness location for NACA 64A-series airfoils $\left(c_l = 0, M = 1.0\right)$ is
compared in figure 11 with the change predicted by the transonic simi-
larity law. The comparison shows that the predicted values are in fair
agreement with experiment. The difference in slopes of the two results
indicates that closer correlation can be obtained by empirically changing
the exponent in the transonic similarity law.

The general applicability of the transonic similarity law to the
prediction of pressure coefficients at chordwise stations other than the
maximum-thickness location can be approximated by inspection of the
pressure distributions for NACA 64A-series airfoils at $c_l = 0$ in fig-
ure 12. The pressure distributions of figure 12 indicate a progressive
change in pressure coefficient with thickness for stations between the
30- and 60-percent-chord locations. The agreement shown in figure 11
for the 39-percent-chord location thus may be considered representative
for all positions between 30- and 60-percent-chord stations. For stations
near the leading or trailing edges, however, experimental pressure distri-
butions show by the nonuniform variation of pressure coefficient with
thickness that the transonic similarity law would not be applicable. The
transonic similarity law is thus of limited applicability.

Supersonic methods.- The empirical method developed by Rainey (refer-
ence 14) may be placed in the third category of using supersonic theory.
The method was presented to be used in the determination of pressure
distributions and forces at supersonic Mach numbers wherein the leading-
edge shock was detached. The method is an application of linearized
theory and normal-shock theory. One characteristic result from linear
theory is that stream velocity $P = 0$ occurs locally on the profile near
the region where the surface tangent is parallel to free-stream direction.

The test results at Mach number 1.0, however, show that stream velocity is encountered at a station well forward of the predicted station (fig. 12). Linear theory was therefore considered inapplicable.

Proposed method for determining effects of thickness.- The problem was studied further and a scheme for estimating the pressure distribution on symmetrical airfoils at zero lift was empirically derived. The method requires first the estimation of the sonic-point location. In the case of the airfoils of the present tests (4- to 12-percent thick), the sonic point was found to be displaced rearward from the leading edge by an amount roughly equal to the maximum thickness (4-percent chord for 4-percent-thick airfoils and 12-percent chord for 12-percent-thick airfoils). It is realized that this rough rule may not hold for other airfoils having widely different nose shapes. The method also required a relation to define the pressure coefficient at a second point on the airfoil surface. The relation was obtained from the transonic similarity law $P = k\left(\dfrac{t}{c}\right)^{2/3}$ at $M = 1.0$ empirically altered to $P_t = -1.52\left(\dfrac{t}{c}\right)^{0.605}_{max}$ for NACA 64A-series airfoils at the maximum-thickness location.

The altered similarity law was used to determine for each of the various profiles at the maximum-thickness station the local Mach number and the corresponding Prandtl-Meyer flow angle for supersonic expansion ν. The angle ν represents the total effective or resultant expansion between the sonic point and the maximum-thickness station on the airfoil. The next step in the method consisted of determining the surface slopes of the airfoil profiles from the airfoil ordinates for chordwise stations between the sonic point and the trailing edge. These surface slopes were referred to the sonic point as the 0° datum and were multiplied by the ratio of the angle ν to the surface slope at the maximum thickness. The adjusted slopes were used in combination with Prandtl-Meyer relations for an expanding supersonic flow to compute variations in pressure coefficient along the airfoils. The resulting pressure distributions were thereby forced to agree with the empirically determined values at the sonic points and at the location of maximum thickness.

Application of proposed method.- The effect of the adjustment to the surface slopes is illustrated in figure 13, which shows variations in pressure coefficient along the chord for the NACA 64A009 airfoil section at 0° angle of attack and Mach number of 1.0. The long- and short-dash curve shows the predicted variation from the sonic point assuming a pure supersonic expansion along the surface or full Prandtl-Meyer turns occurring rearward of the sonic point. The dashed curve shows similar expansion fore and aft of the maximum-thickness location where the pressure

was determined from the empirically altered transonic similarity law.
The solid curve in figure 13 is the estimated pressure distribution
obtained from the altered slopes which required agreement at the sonic
point and at the maximum thickness. It is noted that this estimated
pressure distribution indicates a more rapid expansion just after the
sonic point than was obtained experimentally. Further, it is found that,
around the maximum-thickness location, roughly 40-percent-chord station,
the experimental variation indicates a more rapid expansion than does
the estimated distribution; whereas, near the trailing edge, the esti-
mated pressure coefficients are more negative than those experienced
experimentally. These differences may be attributed to several factors.
Over the forward part of the airfoil, reflections from the sonic boundary
back to the airfoil surface cause compressions and result in a slower
rate of expansion of the experimental flow. The disagreement at the
rear part of the airfoil is attributable to viscous effects which decrease
the effective rate of change of surface slope and at the same time per-
mit the pressures to be propagated upstream through the boundary layer,
thereby influencing the flow.

The pressure distribution between the leading edge and the sonic
point is obtained by fairing the estimated distribution to the stagnation-
pressure coefficient at the zero-percent-chord station. The stagnation-
pressure coefficient can be computed and is 1.276 for $M = 1.0$.

Comparison of experimental and estimated effects of thickness.-
Pressure distributions estimated by the proposed method are shown for
zero lift and compared with experimental values in the upper part of
figure 14 for the NACA 64A-series airfoils varying in thickness from 4
to 9 percent. The symmetrical-airfoil average loading (fig. 9) was used
in conjunction with the estimated zero-lift pressure distributions to
provide estimated pressure distributions at lift coefficients for the
various airfoils. It was assumed that the angle of attack or lift loading
$\left(\frac{\Delta P}{c_l} \text{ multiplied by desired } c_l\right)$ was equally distributed between upper
and lower surfaces. It can be seen that the estimated distribution pro-
vides good correlation for pitching-moment coefficients for the 6- and
9-percent-thick airfoils. For the 4-percent-thick airfoil, the difference
in moment corresponds to less than 5 percent in center-of-pressure loca-
tion. The comparisons indicate that the estimated distributions are in
fairly good agreement with experimental results.

Proposed method for determining pressures on airfoils of different
thickness distributions.- For the other series of airfoils there was insuf-
ficient data for profiles of different thicknesses to evaluate empirically
the terms k and n in the transonic similarity relation $P = k\left(\frac{t}{c}\right)^n$.

From the data on the NACA 64A-series airfoils varying in thickness
(fig. 11), it was found that, for a given chordwise station (not surface
slope), the exponent n was 0.605 ± 0.005 for all positions between the
30- and 60-percent-chord stations. The close correspondence of this
exponent with the theoretical value of 0.667, together with the constancy
of this value for the 64A-series profiles, led to the assumption that the
same value was applicable for profiles having other thickness distributions
(fig. 3(b)). By using the exponent n as 0.605 and experimentally
determined values of the pressure coefficient at the maximum-thickness
locations P_t, the shape factor k was found to change from -1.60 for
NACA 63A009 airfoil to -1.50 for NACA 65A009 airfoil, and to -1.32 for
NACA 16-009 airfoil. The systematic decrease in the numerical value of
k with rearward movement of maximum-thickness location indicated that
the scheme of estimating pressure distributions could be extended to
the other airfoils having somewhat different thickness distributions.

Comparison of experimental and estimated effects of thickness
distribution.- The values of k determined in the preceding section
were used in the proposed method to estimate pressure distributions at
a Mach number of 1.0 and zero lift for the airfoils having thickness
distributions that differed from the NACA 64A-series airfoils. The esti-
mated distributions are compared with experimental values in figure 15.
The symmetrical-airfoil average loading was used as in figure 12 to esti-
mate the pressure distributions for lift coefficients around 0.5 and are
also presented in figure 15. A comparison of the estimated and experi-
mental pressure distributions and the resulting moment coefficients
indicates that the method provides reasonably good agreement with
experiment.

Experimental Loadings on Cambered Airfoils

Effect of camber.- As previously stated, the data available from
the present investigation on cambered airfoils are limited to three pro-
files having variations in camber expressed in terms of design lift coef-
ficients of 0, 0.2, and 0.5. Data near a Mach number of 1.0 only will
be discussed. The flow past the three NACA 64A-series profiles, having
a thickness of 6 percent but differing in design lift coefficient, is
shown in figure 16 at a Mach number of 0.97 and lift coefficient of
approximately 0.3. The major difference appearing in the flow photographs
on the upper surface of the models is that the shock is a little farther
forward for the symmetrical profiles than for the cambered profiles. On
the lower surface, however, the cambered profiles have two shocks. This
multiple-shock appearance is especially prominent on the airfoil cambered
for a design lift coefficient of 0.5. The forward shock shown on this
airfoil can be explained on the basis of observed flow changes.

A decrease in load over the forward part of an airfoil occurs as the Mach number is increased above the critical value because of a reduction in upwash ahead of the airfoil. A reduction in upwash is attributable to a reduction in the influence of the rearward parts of the airfoil on the flow near the leading edge, since local regions of supersonic flow impose limitations on pressure propagation (reference 15). A symmetrical airfoil at an angle of attack experiences, for the aforementioned reasons, a reduction in the aerodynamic angle of attack of the leading edge with increase in Mach number. These flow conditions are favorable toward eliminating separated flow and producing the leading-edge shock formation on the sharp-leading-edge symmetrical airfoils described in reference 16. In the present case, because of curvature of the mean line of the highly cambered airfoils and the moderately low angle of attack (lift coefficient approximately 0.3), the leading-edge part of the profile undergoes an increase in negative aerodynamic angle of attack with increase in Mach number. The resulting flow changes produce only slightly separated flow on the lower surface of the cambered profile before reattachment of flow and the accompanying shock formation occur near the leading edge as the Mach number is increased. The shock formation at the leading edge of the highly cambered airfoil in figure 16 is therefore similar to the leading-edge-flow phenomenon described in reference 16. It also follows that this cambered airfoil would have large negative loadings near the leading edge, as are shown in the load distributions (fig. 17).

Figure 17 shows the load distribution along the chord for the three profiles at each of several lift coefficients and at a Mach number of 0.97. In this figure the loading is expressed only as ΔP, to magnify the effect of change in lift coefficient. The effect of increase in camber is readily seen, for any given lift coefficient, to cause reduction in load near the leading edge with a corresponding increase in load near the trailing edge.

Loadings due to lift on cambered and symmetrical airfoils.- The rearward convergence of the loadings (fig. 17) indicates that the symmetrical-airfoil average loading previously discussed might be applicable to the cambered profiles. In order to check this possibility, the increment in ΔP between curves for each of the cambered profiles has been divided by the difference in lift coefficients for the curves. This lift loading is expressed as $\dfrac{\Delta(\Delta P)}{\Delta c_l}$ and its variation along the chord at a Mach number of 0.97 is shown in figure 18. Some effects of the location of lower-surface shocks on loads, such as are occurring near the 75-percent-chord station on the NACA 64A206 airfoil and around the 10-percent-chord station on the NACA 64A506 airfoil, are evident for these cambered sections. The major differences between the loading due to angle of attack on the cambered profiles and the average loading curve

derived from symmetrical airfoils are attributable to lower-surface shocks, as seen in the flow photographs of figure 16. From these limited data it appears that the effects of camber can be separated from angle-of-attack effects; thus, the effects of camber, angle of attack, and thickness can to a first approximation be treated separately at a Mach number of 1.0 as at both low subsonic Mach numbers and at supersonic Mach numbers.

Scope of Method

Three-dimensional flow.- It is naturally of considerable interest to see how these two-dimensional data may be applied in a practical application which requires three-dimensional flows. Unfortunately, very little data are available whereby a comparison of two- and three-dimensional results may be made at Mach numbers near unity. Some limited unpublished tests of a straight wing of NACA 65-110 profile have been made in flight with the X-1 airplane at a Mach number of 1.0. These pressure-distribution measurements, obtained at the midsemispan station, are presented in figure 19 and compared with the symmetrical airfoil average loading in a manner similar to the comparison in figure 18. In the low-lift-coefficient range (0.37 to 0.60), there is good agreement between the two- and three-dimensional data. In the high-lift-coefficient range (0.60 to 0.76) the large scatter in the three-dimensional data indicates at best only fair agreement.

Mach number extension.- Inasmuch as the two-dimensional results have been presented to give an estimate of loading only at a Mach number of 1.0 and the method of Rainey (reference 14) permits the loading to be estimated within the detached-shock range at Mach numbers around 1.6, the two methods offer a possibility of examining means of estimating the loadings at intermediate Mach numbers. The method of Rainey is shown in reference 14 to be in good agreement with the experimental pressure distributions on an NACA 65-009 airfoil at Mach numbers between 1.6 and 2.4. The experimental loading at a Mach number of 1.6 and a loading computed by Rainey's method at Mach number 1.4 are compared in figure 20 with the symmetrical-airfoil average loading obtained at a Mach number of 1.0. The results indicate that no large changes in loading occur between a Mach number of 1.0 and a Mach number of 1.6 and that inter-polation of loadings for those intermediate Mach numbers would be a relatively simple process.

CONCLUDING REMARKS

From tests on the NACA 16-009 airfoil and on eight airfoils of the NACA 6A series, results have been presented to show that the chordwise

loading due to lift at a Mach number of 1.0 is insignificantly affected by thickness distribution within the range of airfoil shapes presented and only slightly affected by thickness. In addition, a method of estimating the pressure distributions for lifting symmetrical airfoils at a Mach number of 1.0 which seems applicable to profiles of the type considered herein has been presented. Furthermore, the possibility is indicated that the effects of camber, thickness, and angle of attack may be treated separately at a Mach number of 1.0 as they are at low subsonic Mach numbers and at supersonic Mach numbers.

Langley Aeronautical Laboratory
        National Advisory Committee for Aeronautics
                Langley Field, Va.

REFERENCES

1. Theodorsen, Theodore: Theory of Wing Sections of Arbitrary Shape. NACA Rep. 411, 1931.

2. Naiman, Irven: Numerical Evaluation by Harmonic Analysis of the ϵ-Function of the Theodorsen Arbitrary-Airfoil Potential Theory. NACA ARR L5H18, 1945.

3. Habel, Louis W., and Henderson, James H.: Preliminary Investigation of Airfoil Characteristics in the Langley Annular Transonic Tunnel. NACA RM L50E18, 1950.

4. Stack, John: Methods for Investigation of Flows at Transonic Speeds. From: Symposium on Experimental Compressible Flow, Naval Ordnance Lab. Rep. 1133, June 29, 1949.

5. Lindsey, Walter F., and Chew, William L.: The Development and Performance of Two Small Tunnels Capable of Intermittent Operation at Mach Numbers between 0.4 and 4.0. NACA TN 2189, 1950.

6. Goldstein, S., and Young, A. D.: The Linear Perturbation Theory of Compressible Flow, with Applications to Wind-Tunnel Interference. R. & M. No. 1909, British A.R.C., 1943.

7. Guderley, Gottfried, and Yoshihara, Hideo: The Flow over a Wedge Profile at Mach Number One. Tech. Rep. No. 5783, ATI No. 57842, Air Materiel Command, U. S. Air Force, July 1949.

8. Greene, Leonard Michael: The Attenuation Method for Compressible Flow Systems. Jour. Aero. Sci., vol. 12, no. 3, July 1945, pp. 329-338.

9. Tsien, Hsue-shen, and Fejer, Andrej: A Method for Predicting the Transonic Flow over Airfoils and Similar Bodies from Data Obtained at Small Mach Numbers. GALCIT Rep., Dec. 31, 1944. (Submitted in Partial Fulfillment of Compressibility Effect Project, Contract No. W 33-038 ac-1717 (11592).)

10. Nitzberg, Gerald E., and Sluder, Loma E.: An Empirically Derived Method for Calculating Pressure Distributions over Airfoils at Supercritical Mach Numbers and Moderate Angles of Attack. NACA RM A7B07, 1947.

11. Guderley, K. Gottfried: Singularities at the Sonic Velocity (Project No. HA-219). Tech. Rep. No. F-TR-1171-ND, ATI No. 23965, Air Materiel Command, U. S. Air Force, June 1948.

12. Von Kármán, Theodore: The Similarity Law of Transonic Flow. Jour.
    Math. and Phys., vol. XXVI, no. 3, Oct. 1947, pp. 182-190.

13. Kaplan, Carl: On Similarity Rules for Transonic Flows. NACA
    Rep. 894, 1948. (Formerly NACA TN 1527.)

14. Rainey, Robert W.: Pressure Measurements at Supersonic Speeds on
    a Section of a Rectangular Wing Having an NACA 65-009 Profile. NACA
    RM L9L16, 1950.

15. Lindsey, W. F.: Effect of Compressibility on the Pressures and
    Forces Acting on a Modified NACA 65,3-019 Airfoil Having a 0.20-Chord
    Flap. NACA ACR L5G31a, 1946.

16. Lindsey, W. F., Daley, Bernard N., and Humphreys, Milton D.: The
    Flow and Force Characteristics of Supersonic Airfoils at High Sub-
    sonic Speeds. NACA TN 1211, 1947.
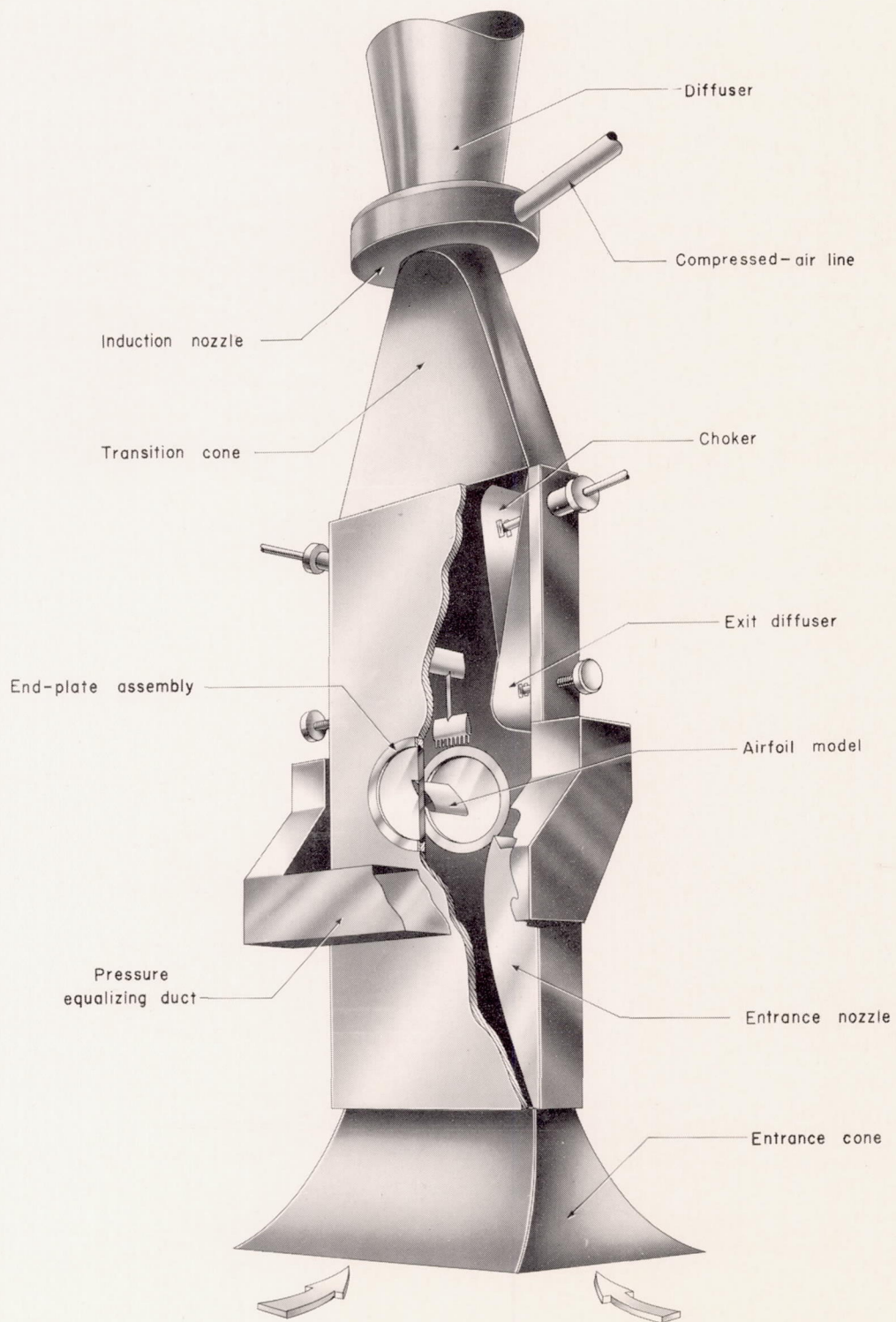
Figure 1.- Configuration of the Langley 4- by 19-inch semiopen tunnel.
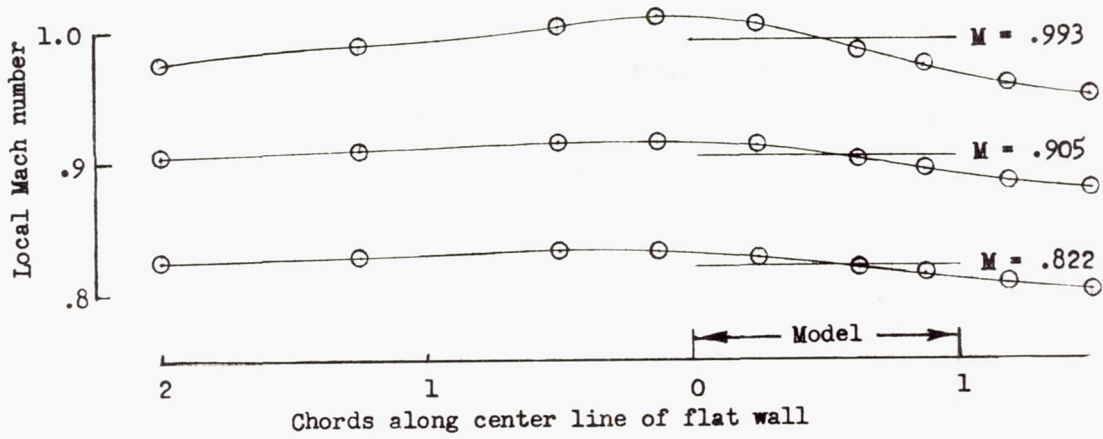
(a) Chordwise Mach number distribution.
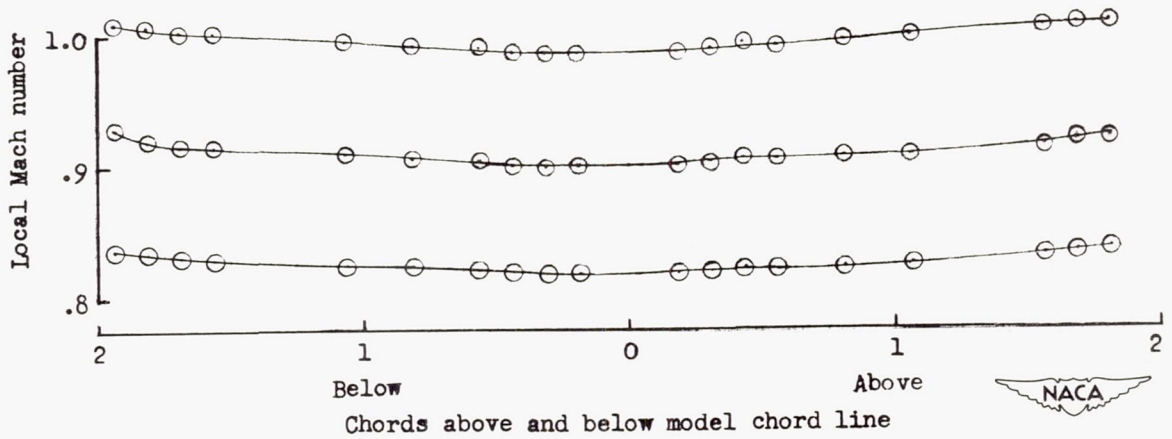
(b) Normal-to-chord Mach number distribution.

Figure 2.- Mach number distribution in the Langley 4- by 19-inch semiopen
tunnel.

Location of maximum t/c

NACA

64A004 airfoil

64A006 airfoil

64A009 airfoil

NACA

64₁A012 airfoil
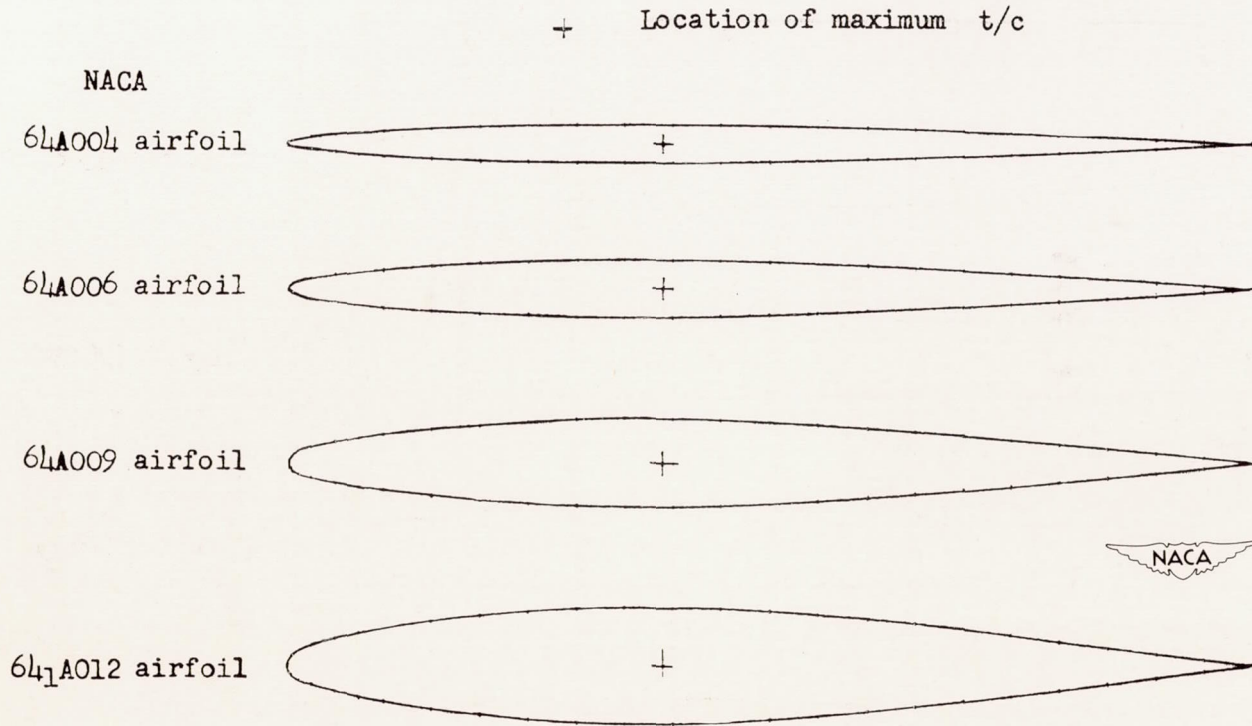
(a) Thickness variation.

Figure 3.- Airfoil profiles.

+ Location of maximum t/c

NACA

63A009 airfoil

64A009 airfoil

65A009 airfoil

16-009 airfoil
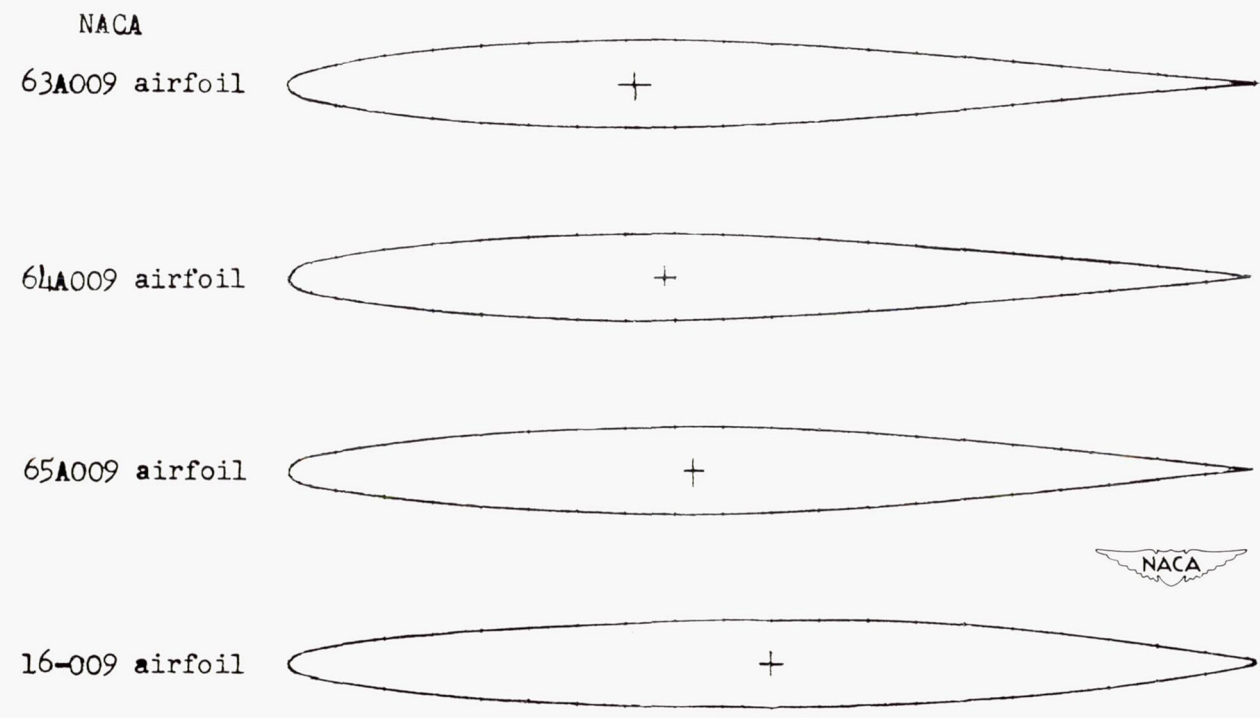
(b) Changes in shape.

Figure 3.- Continued.

NACA
64A006 airfoil

Camber line

64A206 airfoil

NACA

64A506 airfoil
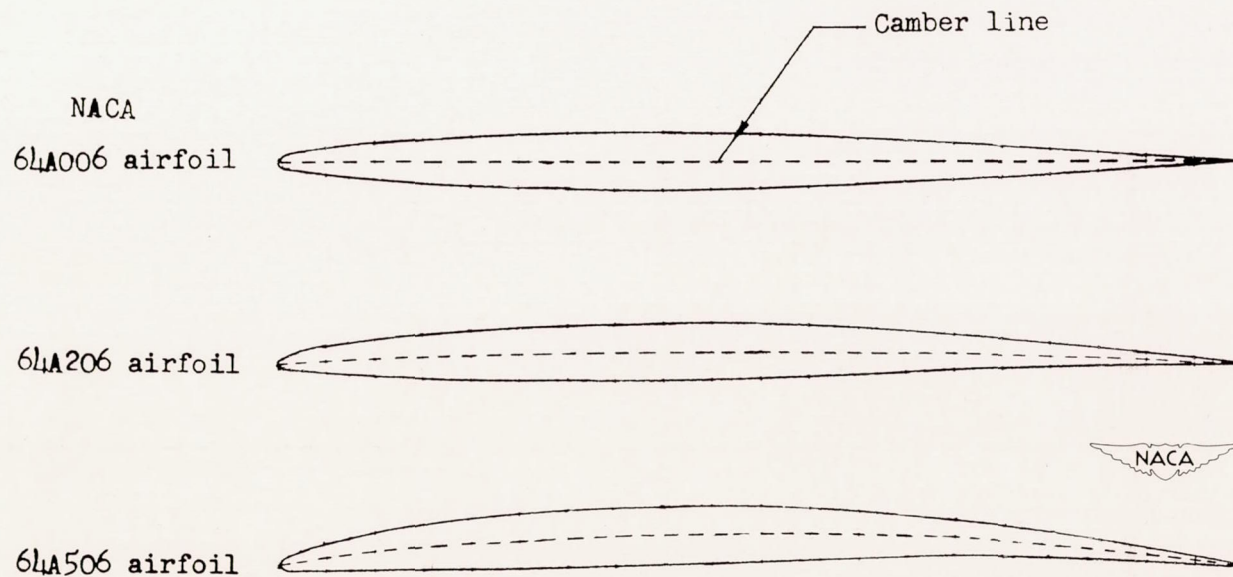
(c) Camber variation.

Figure 3.- Concluded.
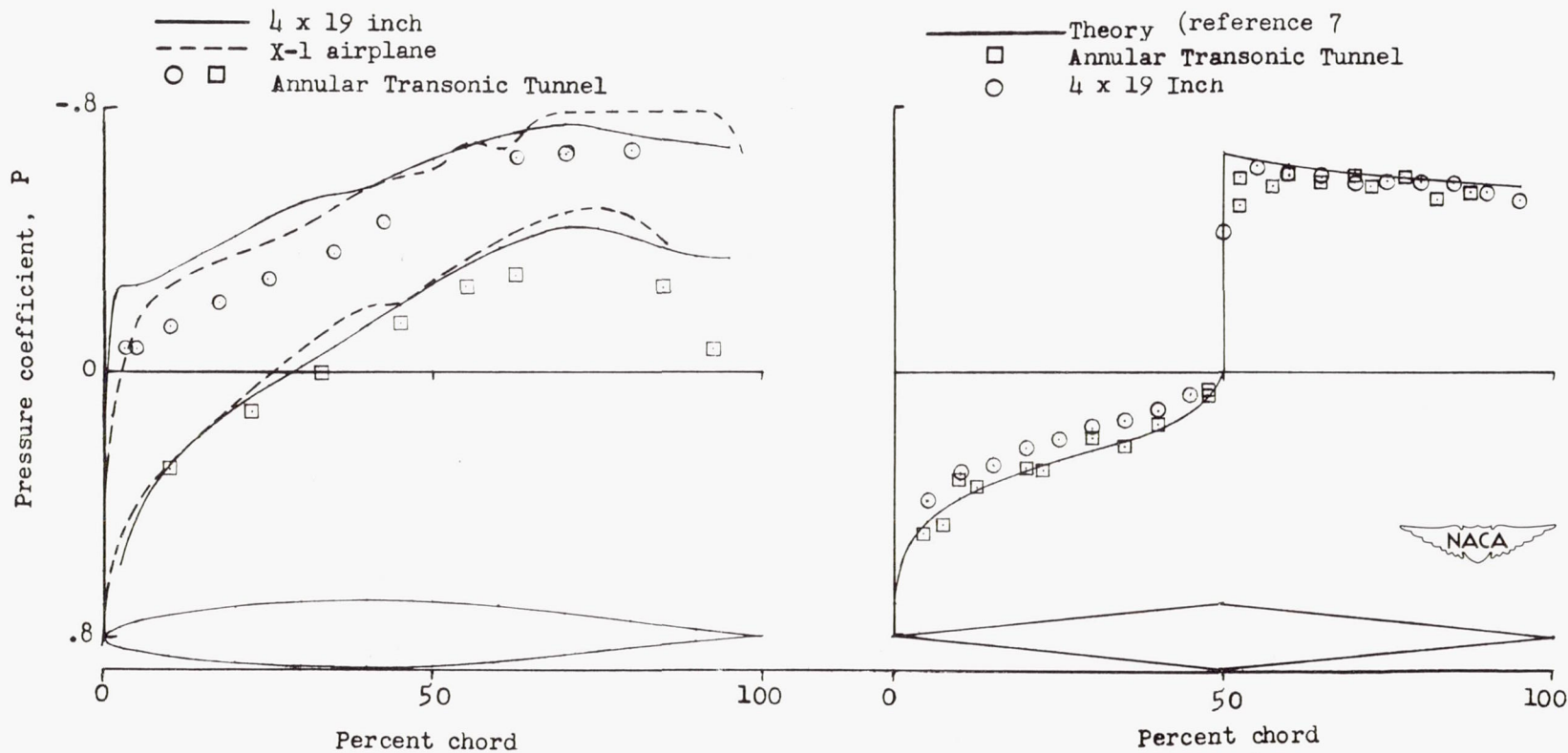
(a) NACA 65-110.
$c_l \approx 0.4$.

(b) 10-percent-thick symmetrical
wedge. $c_l = 0$.

Figure 4.- Comparison of pressure distribution obtained in Langley 4- by
19-inch semiopen tunnel at $M = 1.0$ with those obtained by other
methods.
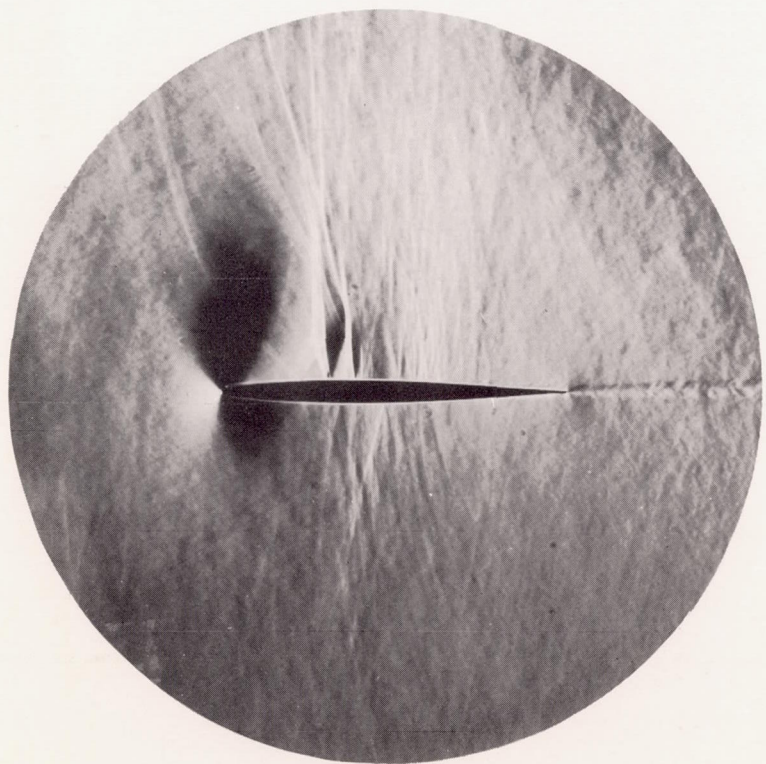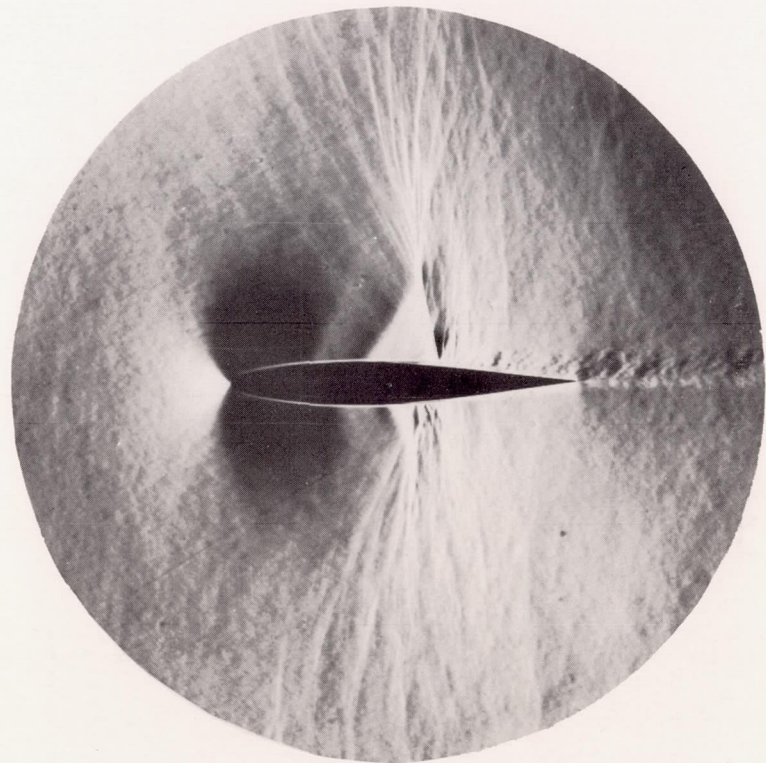
NACA 64A006   NACA 64₁A012

(a) M = 0.82.

Figure 5.- Effect of thickness on flow $c_l \approx 0.2$.   L-72670
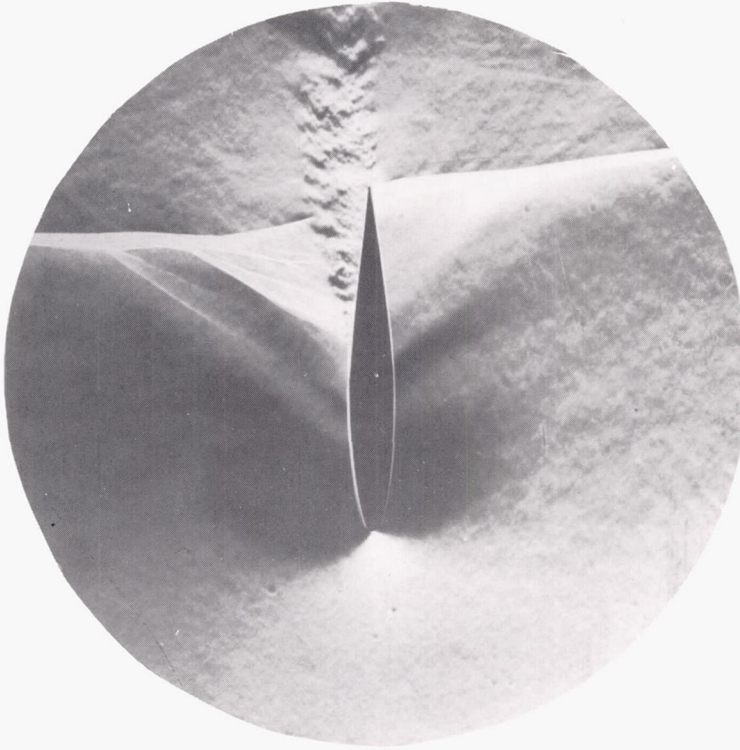
NACA 64₁A012

L-72671

NACA 64A006

(b) M = 0.91.

Figure 5.- Continued.
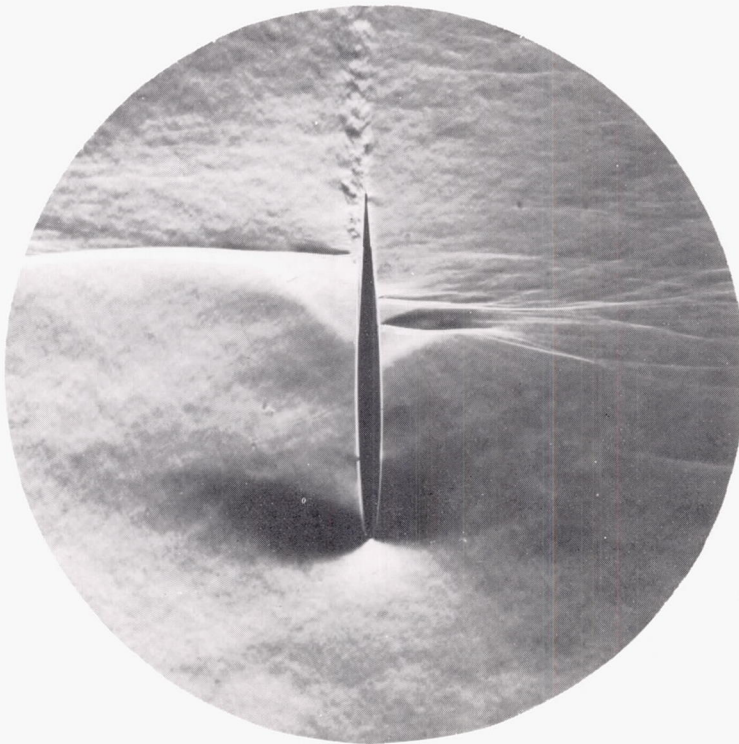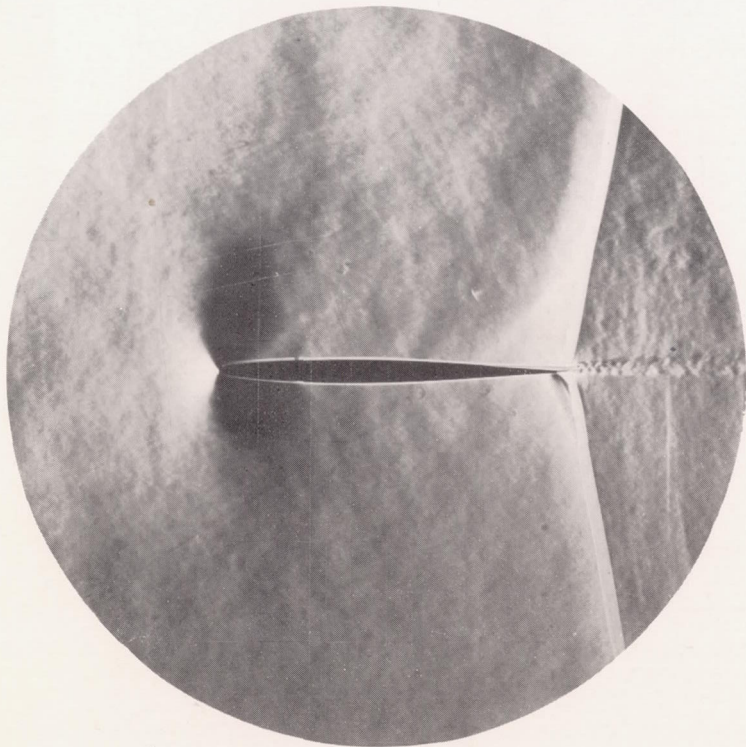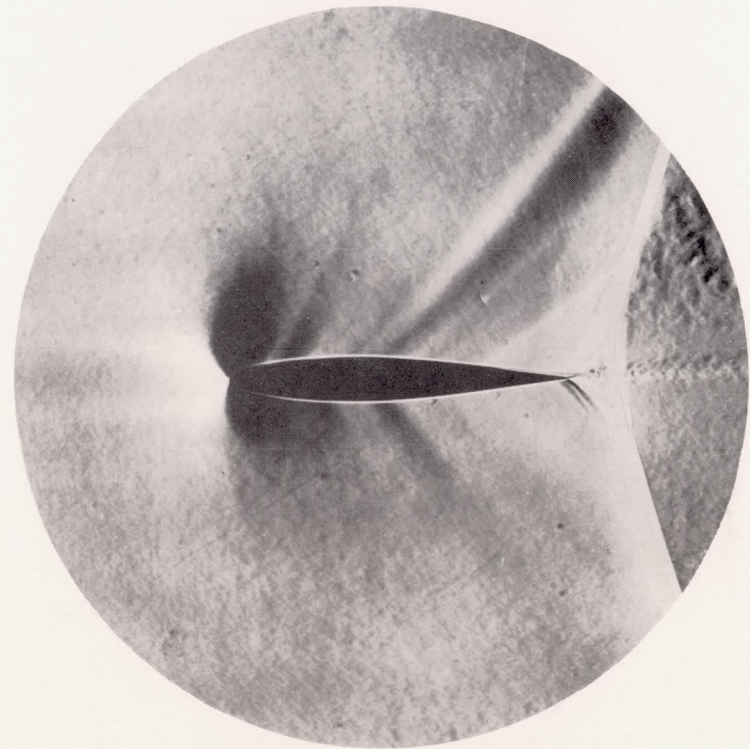
NACA 64A006   NACA 64₁A012

(c) M = 1.0.

Figure 5.- Concluded.
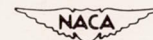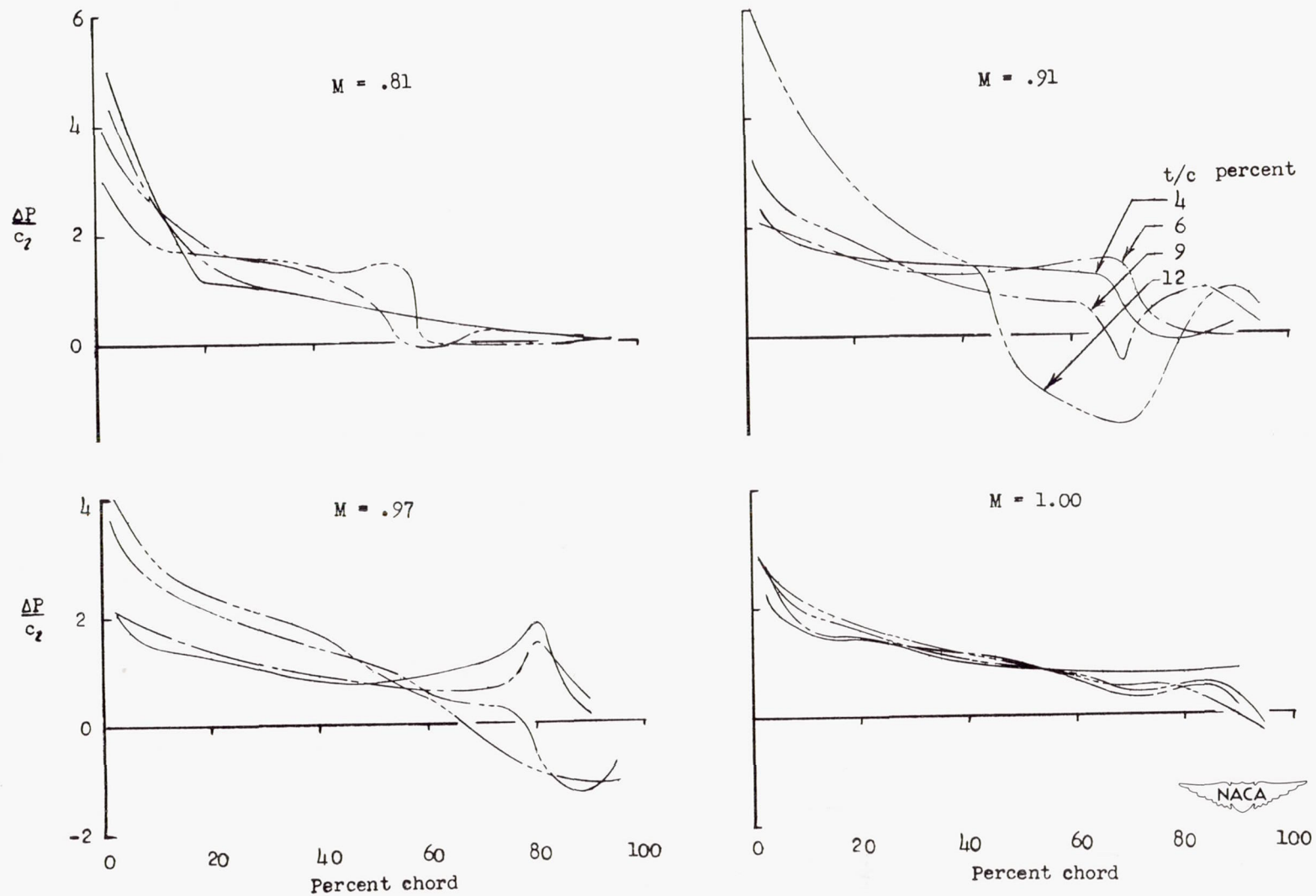
NACA

L-72672

Figure 6.- Effect of thickness on the loading of NACA 64A-series
symmetrical profiles at $c_l = 0.2$.
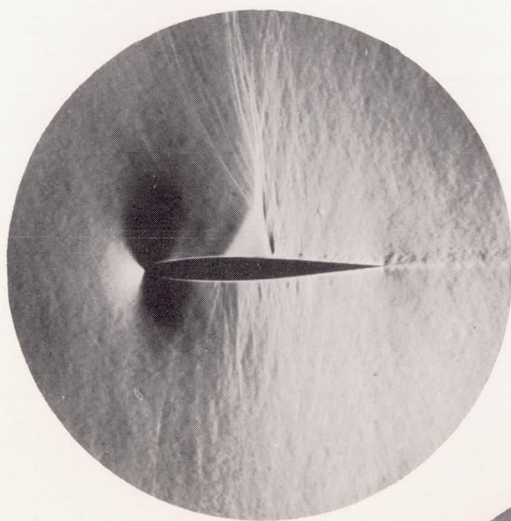
NACA 16-009
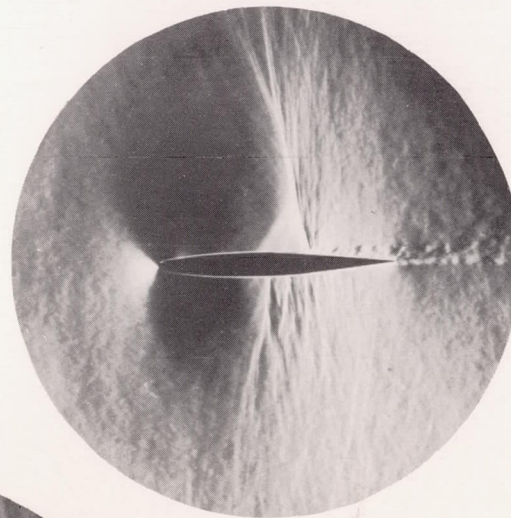
NACA 63A009
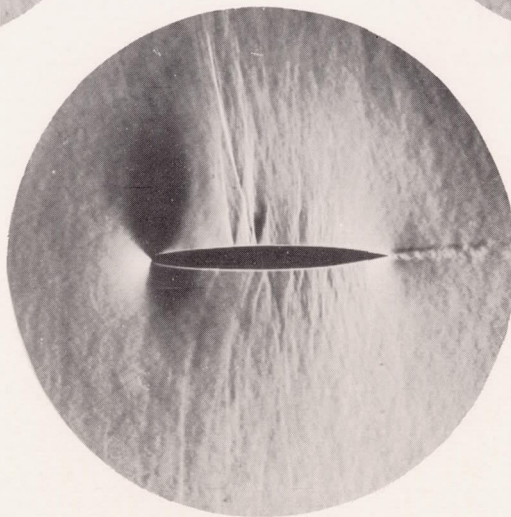
NACA 65A009

(a)   M = 0.82; $c_l \approx 0.23$.
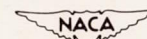
L-72673

Figure 7.- Flow past airfoils of different thickness distribution.
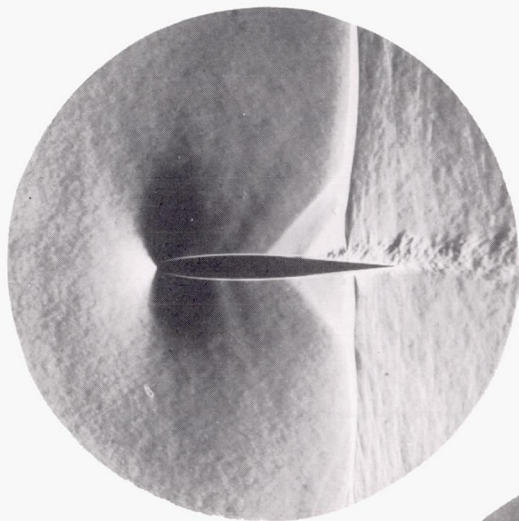
NACA 16-009
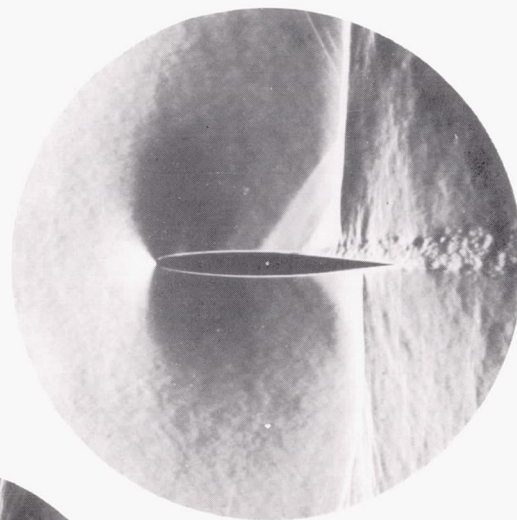
NACA 63A009
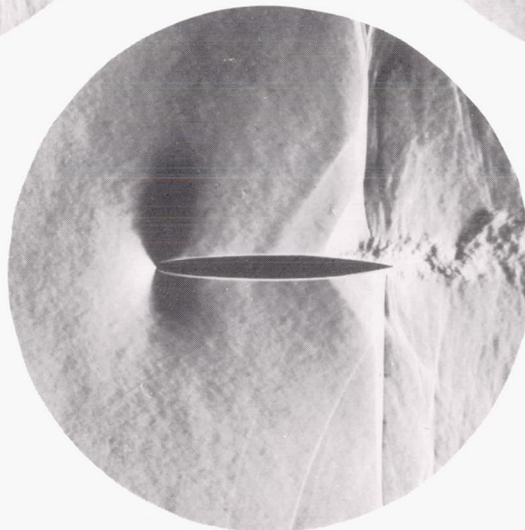
NACA 65A009

(b) $M = 0.92$; $c_l \approx 0.13$.

Figure 7.- Continued.

L-72674
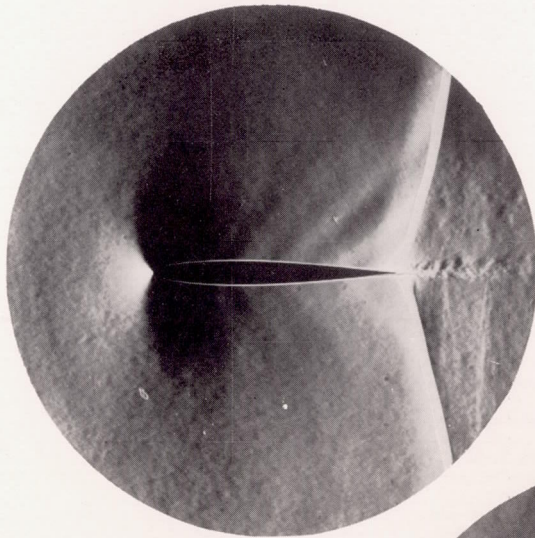
NACA 16-009
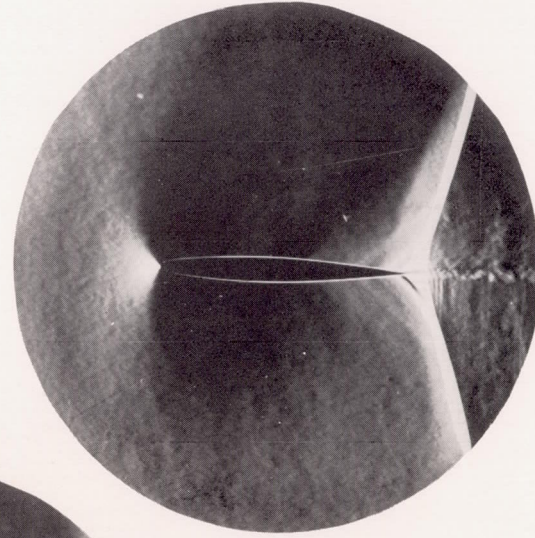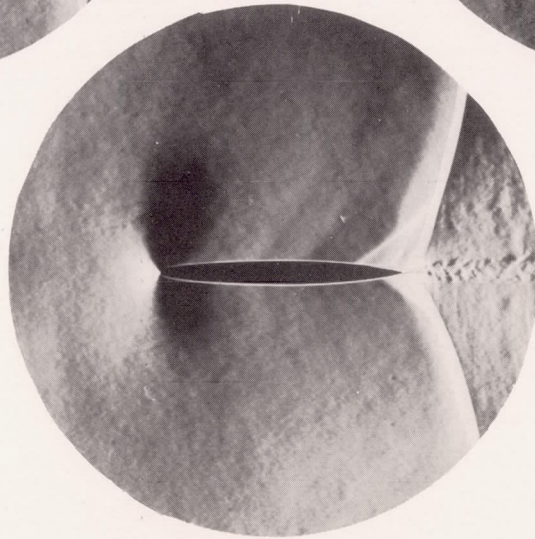
NACA 63A009   NACA 65A009

(c) M = 1.0; $c_l \approx 0.17$.

Figure 7.- Concluded.

L-72675
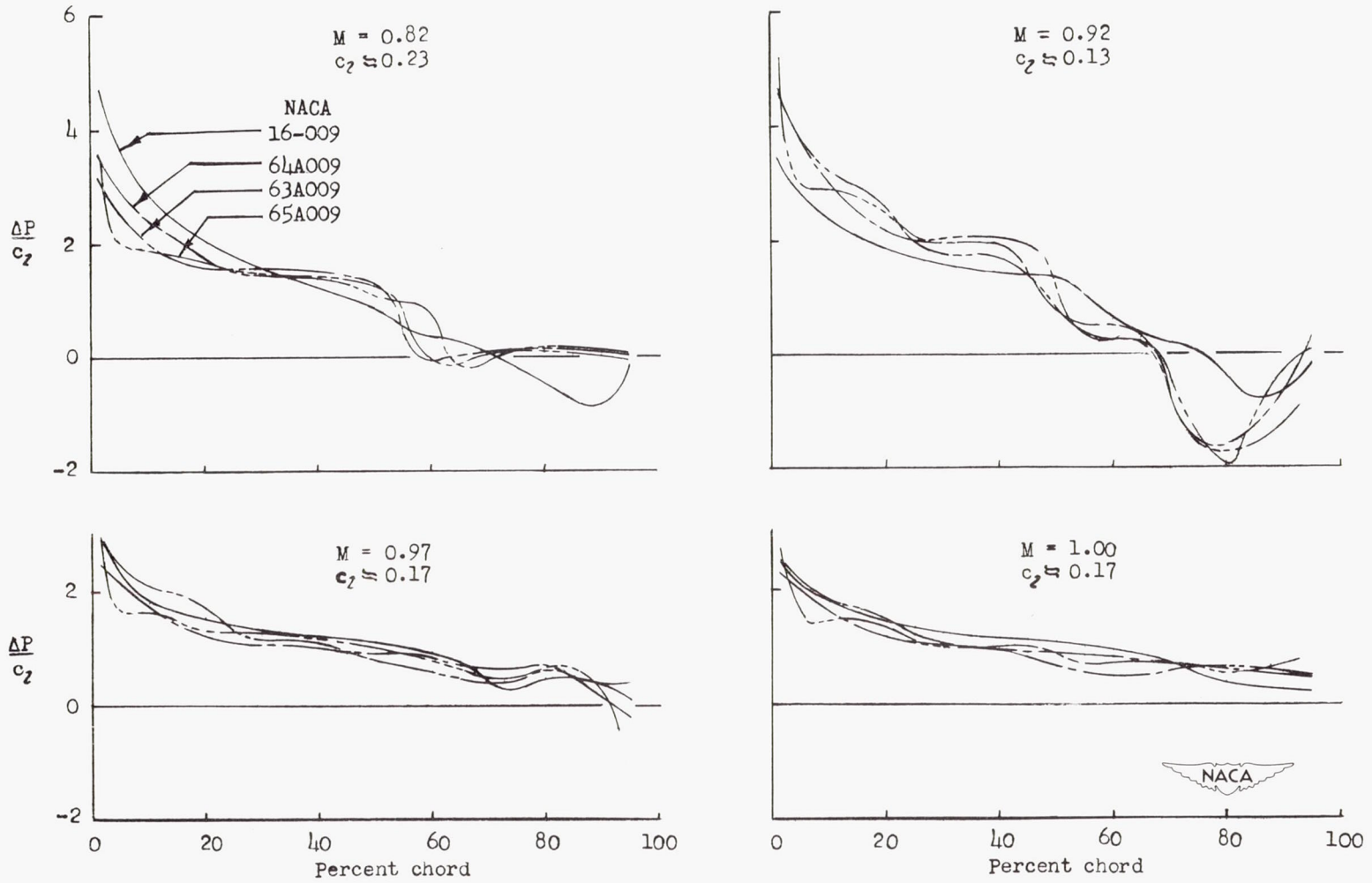
Figure 8.- Effect of thickness distribution on the loading of 9-percent-thick airfoils.
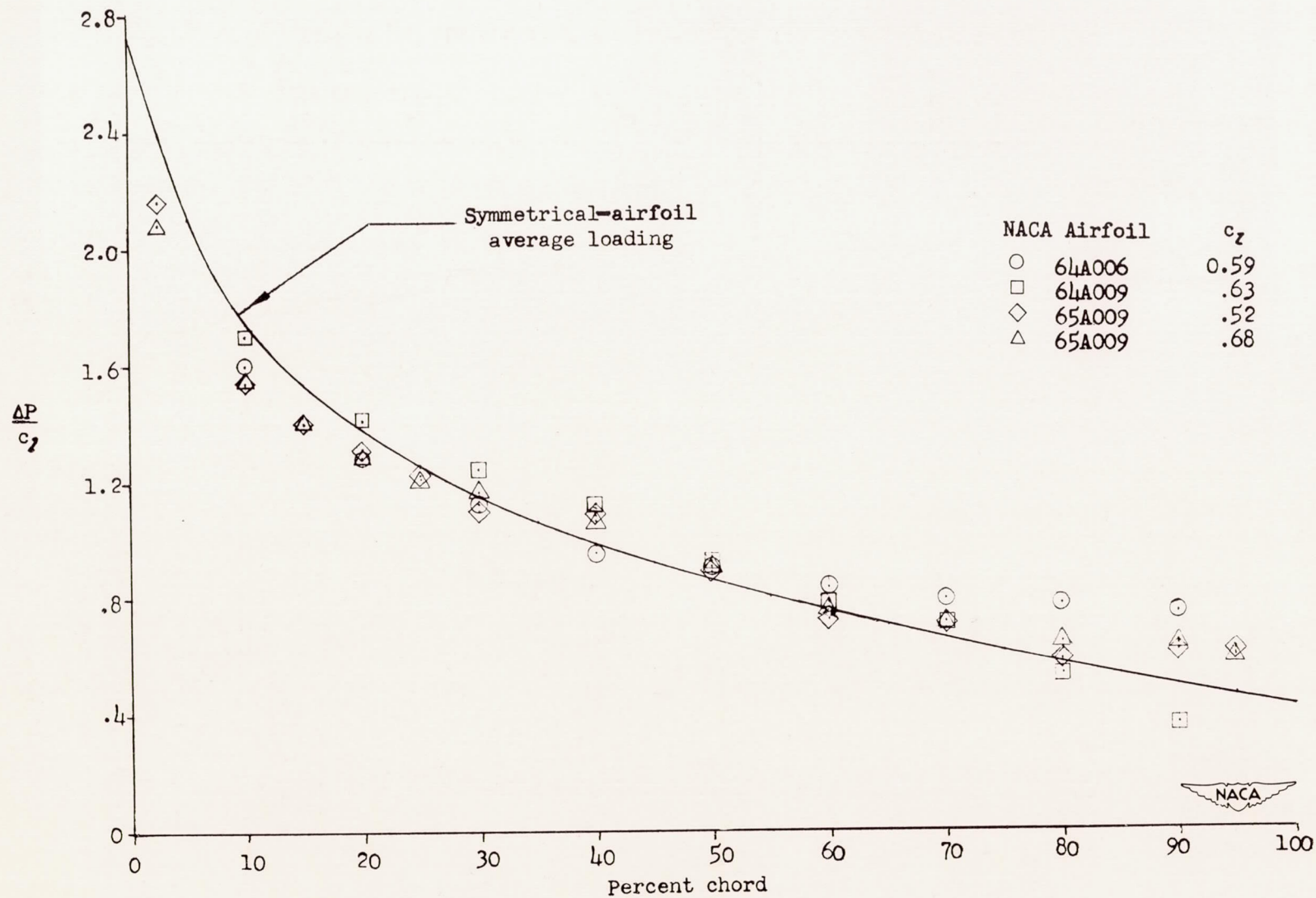
Figure 9.- Symmetrical-airfoil average loading at M = 1.0.
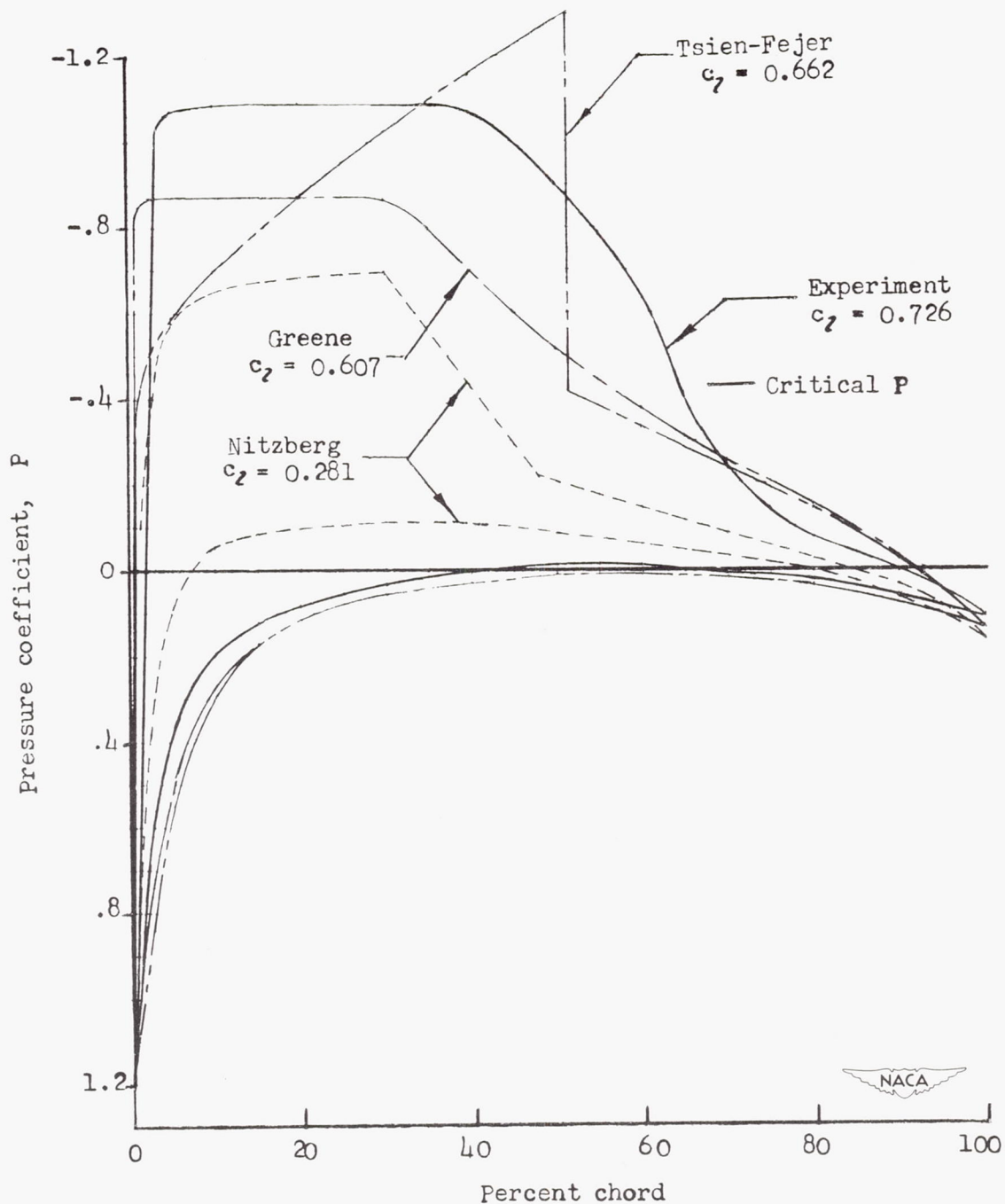
Figure 10.- Comparison of experiment with estimated pressure distribution for NACA 0006. $\alpha = 4°$; M = 0.80.
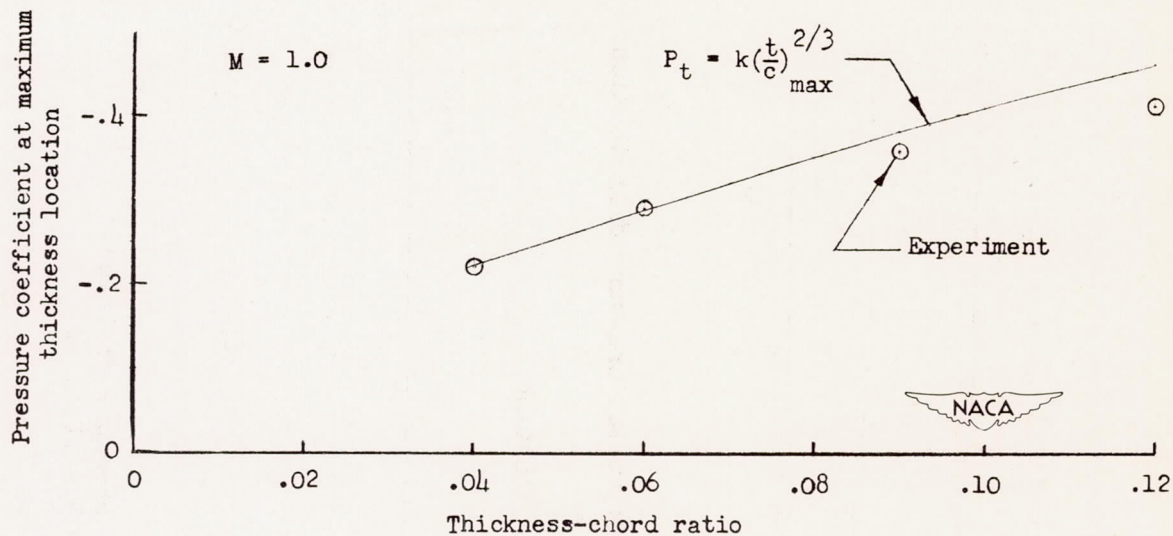
Figure 11.- Comparison of the pressure coefficients at the maximum-thickness location as predicted by the transonic similarity law with those obtained experimentally on the NACA 64A-series symmetrical airfoils.
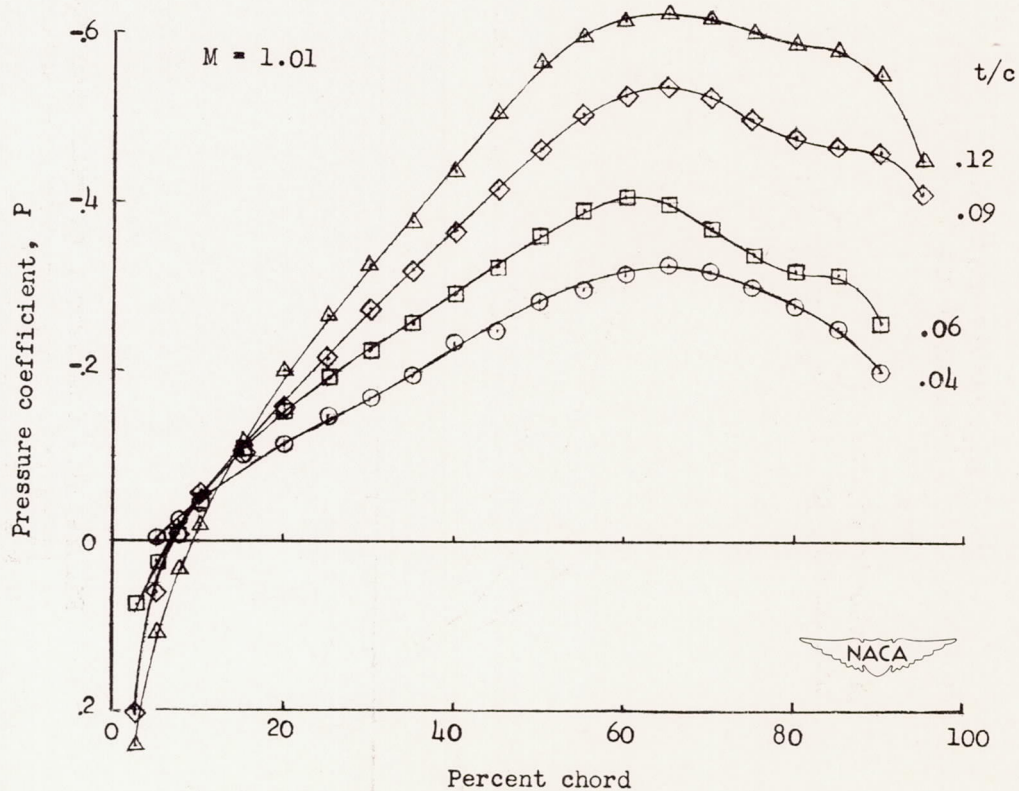
Figure 12.- Effect of thickness on the zero-lift pressure distribution of the NACA 64A-series profiles.
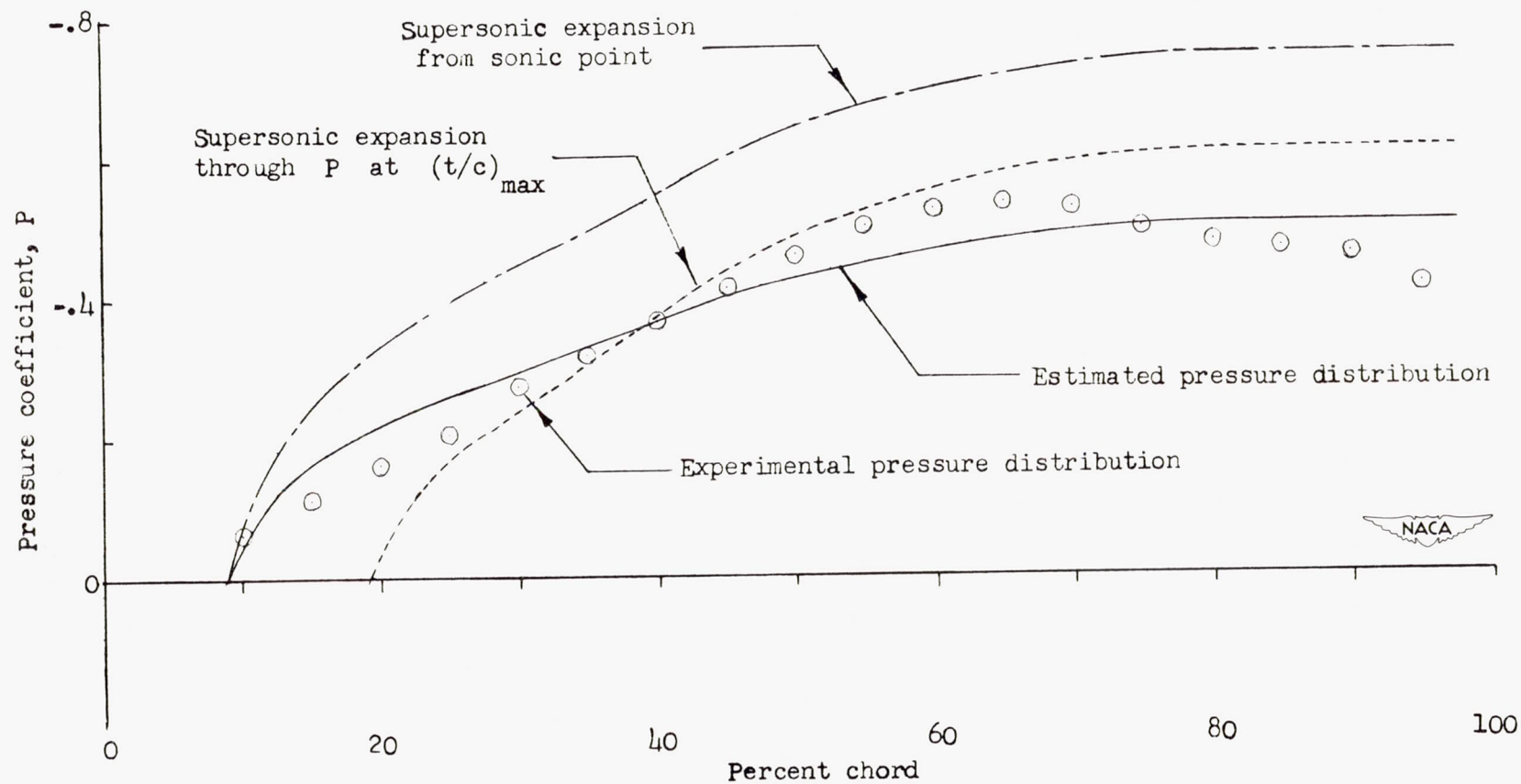
Figure 13.- Comparison of estimated and experimental pressure distributions with pure supersonic expansions. NACA 64A009 airfoil at M = 1.0 and $\alpha = 0°$.
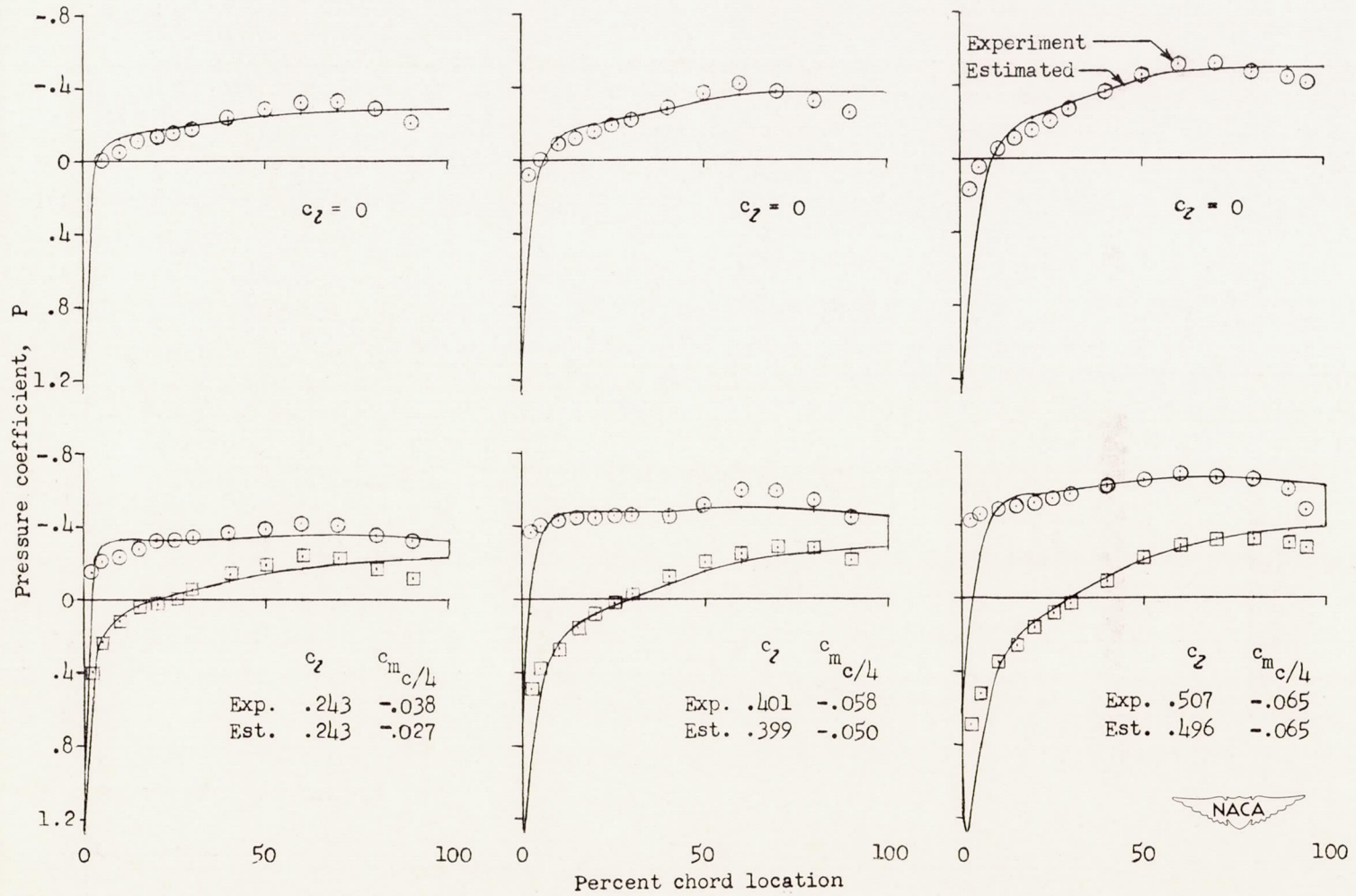
(a) NACA 64A004 airfoil.   (b) NACA 64A006 airfoil.   (c) NACA 64A009 airfoil.

Figure 14.- Comparison of estimated and experimental pressure distributions for three airfoils differing only in maximum thickness. M = 1.0.

Pressure coefficient, P

-.8

-.4

0

.4

.8

1.2

$c_l = 0$

$c_l = 0$

Experiment
Estimated

$c_l = 0$

-.8

-.4

0

.4

.8

1.2

	c_l	$c_{m_{c/4}}$
Exp.	.521	-.080
Est.	.516	-.066

	c_l	$c_{m_{c/4}}$
Exp.	.521	-.074
Est.	.512	-.066

	c_l	$c_{m_{c/4}}$
Exp.	.545	-.061
Est.	.537	-.070

0   50   100

0   50   100

0   50   100

Percent chord location
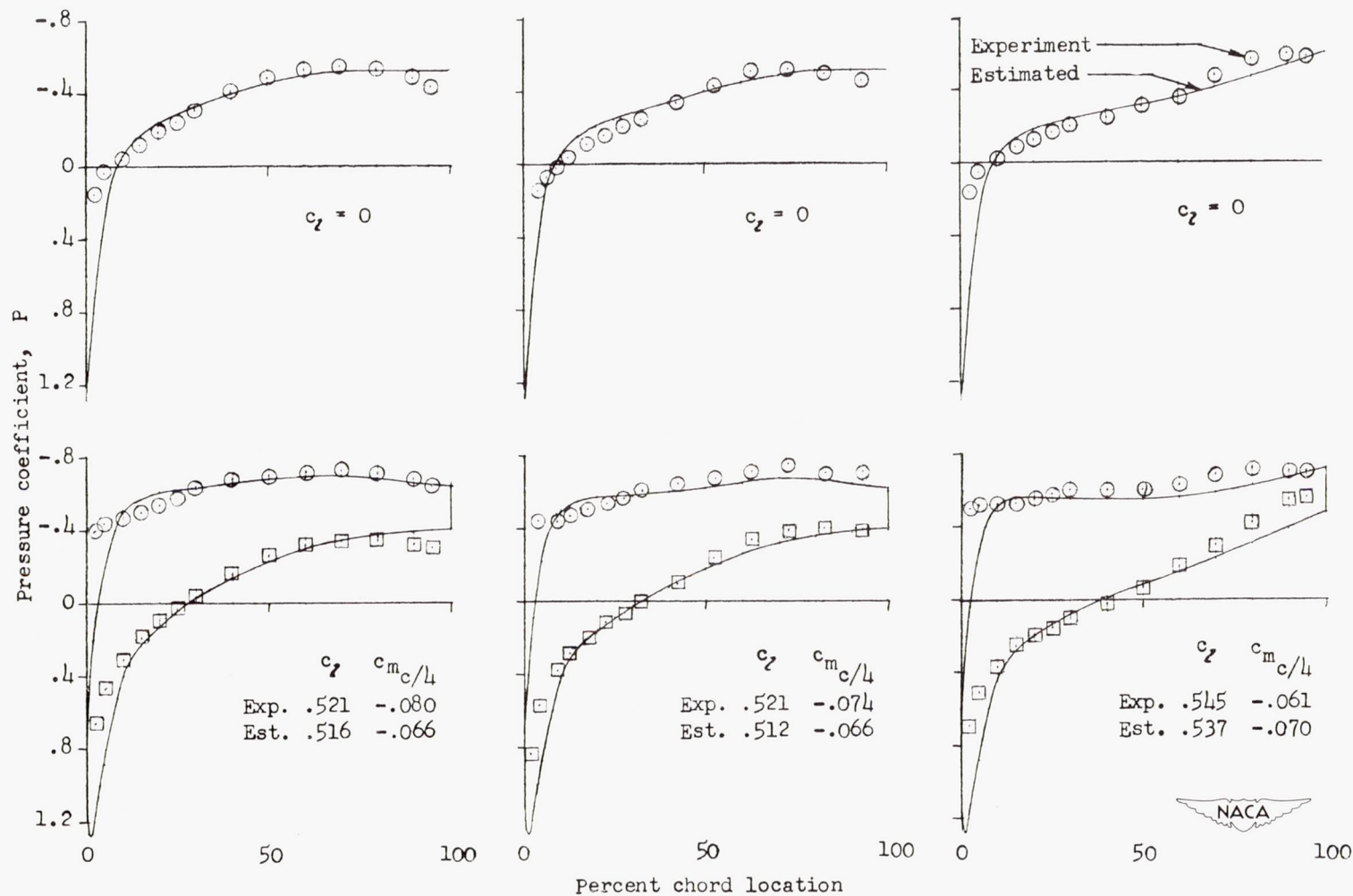
NACA

(a) NACA 63A009 airfoil.   (b) NACA 65A009 airfoil.   (c) NACA 16-009 airfoil.

Figure 15.- Comparison of estimated and experimental pressure distributions
for three airfoils differing in thickness distribution. M = 1.0.
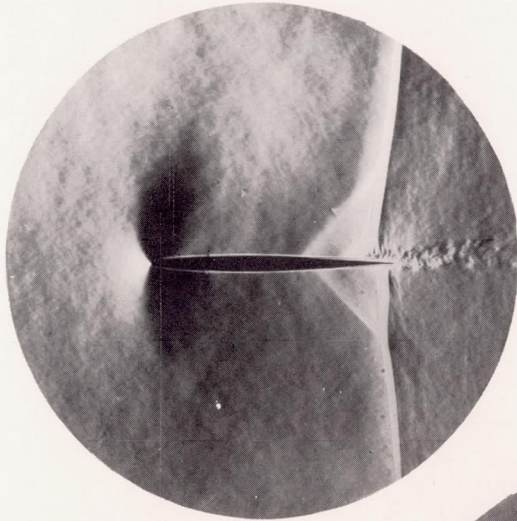
NACA 64A006
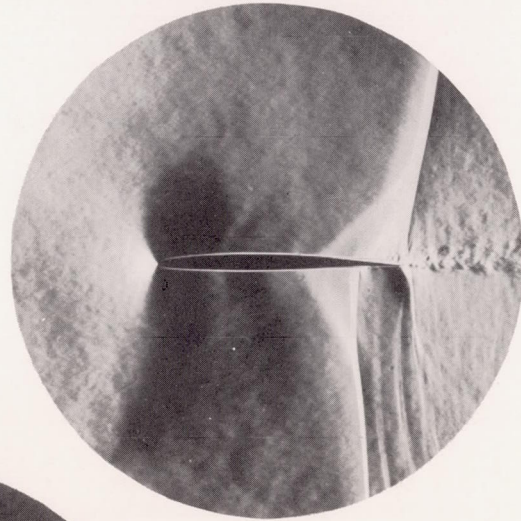
NACA 64A206
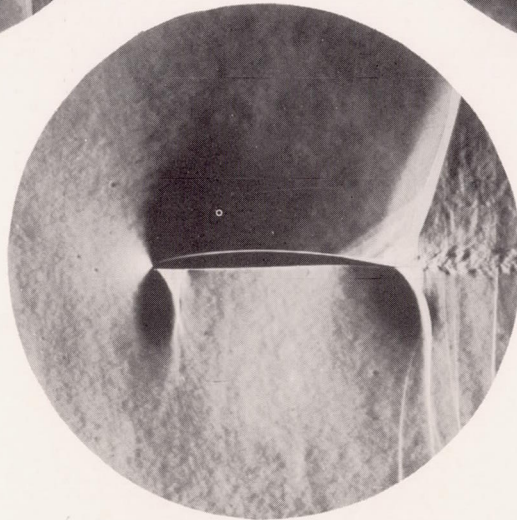
NACA 64A506

L-72676

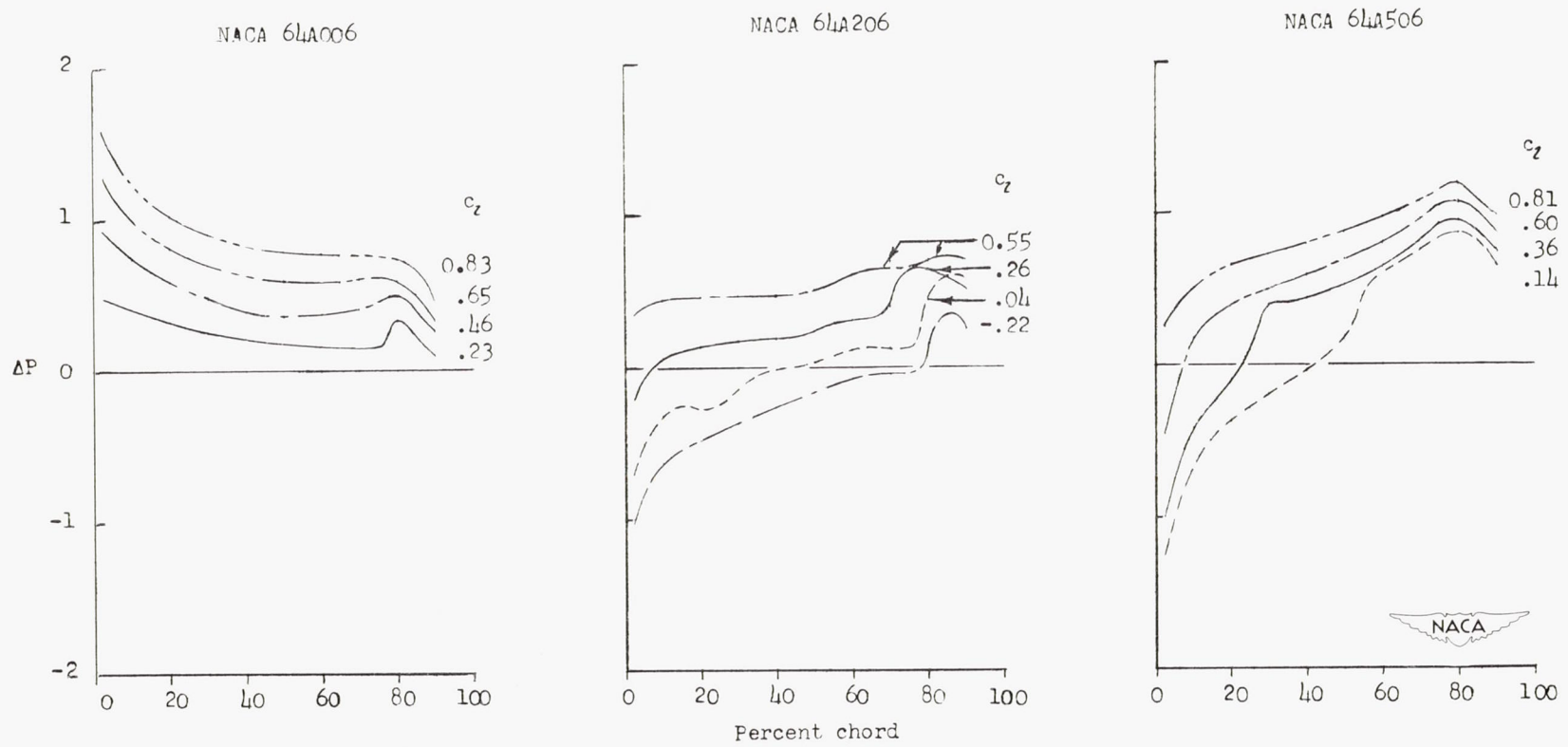Figure 16.- Flow past airfoil as influenced by camber. $M = 0.97$; $c_l \approx 0.3$.

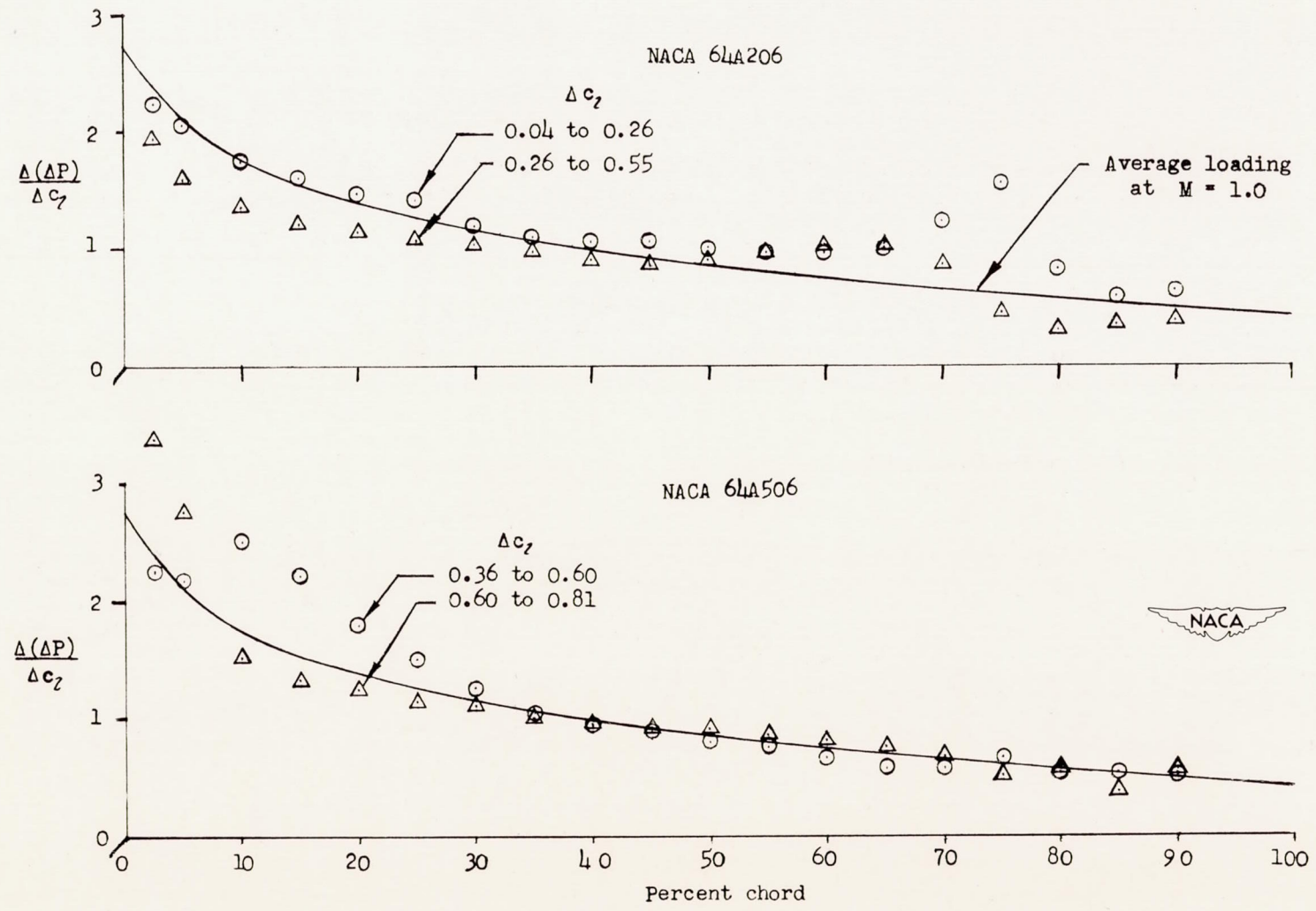Figure 17.- Load distribution on cambered profiles at M = 0.97.

Figure 18.- Comparison of loading due to lift on 6-percent-thick
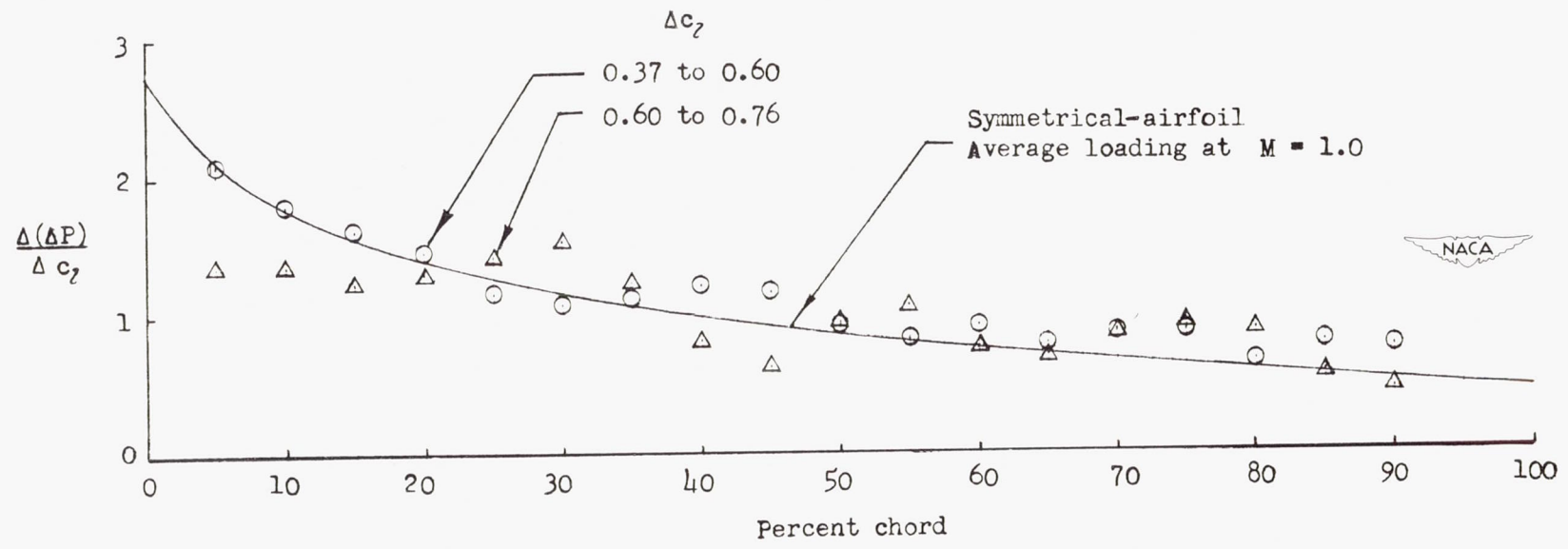cambered sections with the symmetrical-airfoil average loading.
M = 0.97.

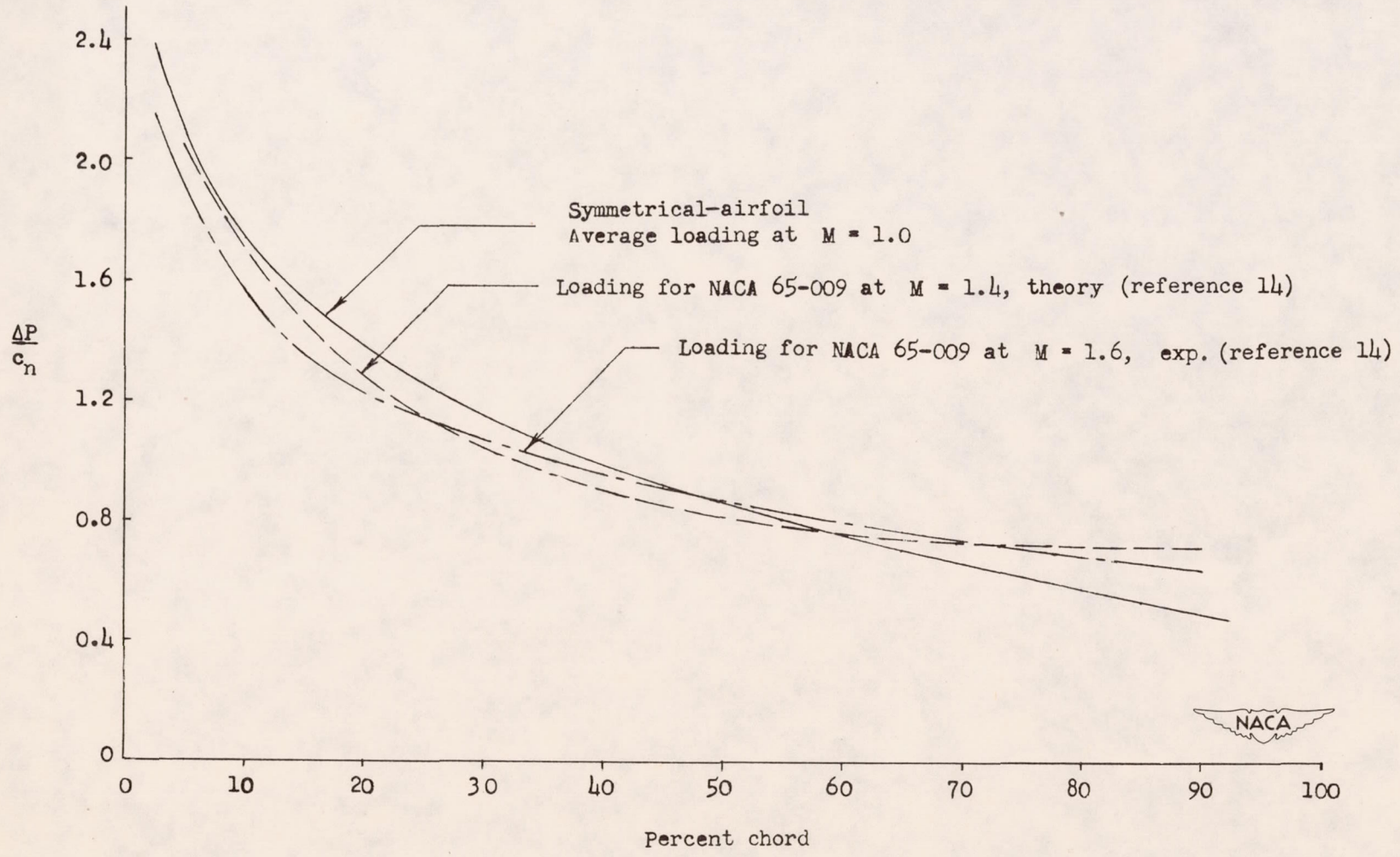Figure 19.- Comparison of loading due to lift on an NACA 65-110 wing section with the symmetrical-airfoil average loading. M = 1.00.

Figure 20.- Effect of change in Mach number on loading.